MODELING, SYSTEM ANALYSIS AND CONTROL OF

A PROTON EXCHANGE MEMBRANE FUEL CELL

by

SUDARSHAN KOLAR

A thesis submitted to the

Graduate School-New Brunswick

Rutgers, The State University of New Jersey

In partial fulfillment of the requirements

For the degree of

Master of Science

Graduate Program in Electrical and Computer Engineering

Written under the direction of

Professor Zoran Gajić

And approved by

_____

_____

_____

New Brunswick, New Jersey

October, 2016

ABSTRACT OF THE THESIS

Modeling, System Analysis and Control of A Proton Exchange Membrane Fuel Cell

by Sudarshan Kolar

Thesis Director:
Professor Zoran Gajić

This thesis presents a control technique for a 9th-order linearized Proton Exchange Membrane fuel cell model. This work starts with giving a brief introduction about the construction and working of PEM fuel cell. Then, various fuel cell subsystems and their corresponding non-linear dynamical equations are presented. These equations are simulated to obtain steady state operating points of the model which is further used in Jacobian linearization. The linearized model consists of nine states as opposed to the eight states of the linearized model available in the literature. A pole placement controller is designed for the linearized model to obtain desired transient performance. This work concludes with inspiring the readers about some future works that can be carried out on this model.

Acknowledgements

I would like to express heartfelt gratitude to Prof. Zoran Gajić. I learnt a lot under his tutelage and more importantly the learning was insightful. I would like to dedicate this thesis to him, because without his supervision the thesis might never have reached it's culmination.

My sincerest thanks to my undergraduate advisor Dr. Prasheel Suryawanshi, who offered all his guidance during my pursuit of Master's degree all the way from India.

I feel blessed to have been a student of some of the elite faculties of our university, Prof. Zoran Gajic, Prof. Lawrence Rabiner, Prof. Kristin Dana, Prof. Jerrold Tunnell and Prof. Abraham Borno. I learnt a great deal from all your courses and I will miss your class.

Thanks to the committee members Prof. Hana Godrich, Prof. Prasheel Suryawanshi and Prof. Zoran Gajić for taking time out of your busy schedule and for your encouragement.

A big thank you to my seniors Heojong Yoo and Kliti Kodra and friends Gayatri Powar, Remya Ramakrishnan and Saie Saraf for all the inputs and for being great friends during my journey.

Finally, I would like to bow down to my parents and the divine for all the love and support.

Table of Contents

List of Figures

Chapter 1

Introduction

Fuel cells were developed around mid 19th century by Sir William Grove. The principle of operation, however, is believed to be discovered by Friedrich Schonbein [1, 2]. Over the last few decades, fuel cell research is in boom, owning to the environmental impacts of the fossil fuels and their fast depletion. The advantage with fuel cell is obvious. It feeds on oxygen and hydrogen gases and generates clean electrical energy with water as by-product of the reaction. Since fuel cells convert chemical energy directly into electrical energy, it has higher efficiency in comparison to conventional heat engines [3].

The fuel cells were first employed by NASA in their Gemini Program in early 1960s. Fuel cells were also employed in Apollo Program to support guidance and communication [1]. Today, fuel cells are used in many applications from automobiles, power generation, heating to various space programs. Undeniably, fuel cells are the future of renewable energy.

1.1 Fuel Cells: Principle, Construction and Working

1.1.1 Principle of Operation

Fuel cells are electrochemical devices that convert chemical energy into electricity, without generating carbon-dioxide. The operation principle of fuel cells is exactly opposite to that of water electrolysis. In water electrolysis electric energy is supplied to dissociate water into constituent hydrogen and oxygen. In fuel cells, oxygen and hydrogen are made to react to form water, hence releasing electrical energy during the process.

1.1.2 Construction

The construction of a fuel cell is very similar to a triode. It consists of an anode, membrane and cathode. Based on the material of the membrane , there are 6 different classifications of fuel cells presented below [1].

1. Alkaline fuel cells (AFCs);

2. Proton Exchange Membrane or Polymer Electrolyte Membrane fuel cells (PEM-FCs);

3. Phosphoric Acid fuel cells (PAFCs);

4. Molten Carbonate fuel cells (MCFCs);

5. Solid Oxide fuel cells (SOFCs);

6. Direct Methanol fuel cells (DMFCs).

Out of the above, following fuel cells are predominantly used in practice:

1. **PEM fuel cells.** PEM stands for proton exchange membrane. It is also called polymer electrolyte membrane. The membrane is solid, teflon like material and is an excellent conductor of protons and isolates electrons.

2. **SOFC.** SOFC stands for solid oxide fuel Cells. The membrane is made up of ceramic type metal oxide. These membranes are excellent conductors of negatively charged ions (electrons).

PEM fuel cells are the most developed and the best understood types of fuel cells and are gaining popularity in the automobile applications. SOFCs are pre-dominantly being researched for distributed electric power generations.

Some of the significant features of the PEM fuel cells are

1. Long cell life;

2. Low corrosion;

3. High power density of around 2000Wh/Kg;

4. Low operating temperatures;

5. Higher energy conversion efficiency of around 50% against 25% of internal combustion engines.

1.1.3 Basic Operation of PEM Fuel Cells

A PEM fuel cell is presented below in Figure 1.1 The chemical reactions taking place
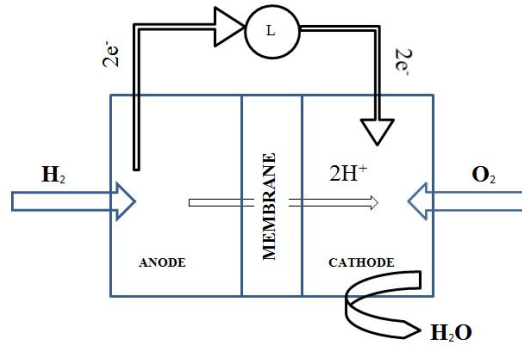
Figure 1.1: Operating Principle of PEM Fuel Cell

in a PEM fuel cell are represented by

$$2\,H_2 \longrightarrow 4\,H^+ + 4\,e^- \text{ (Anode)}$$
$$4\,H^+ + 4\,e^- + O_2 \longrightarrow 2\,H_2O \text{ (Cathode)}$$
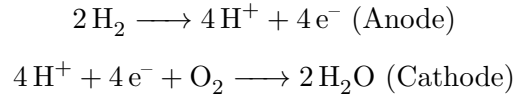
The membrane, being a electron isolator, forces electrons to flow through the load, generating electric current. Water is the by-product of a fuel cell chemical reaction.

1.1.4 V-I Characteristics

The V-I characteristics of a fuel cell is illustrated in Figure 1.2. The fuel cell characteristics deviates from the ideal one because of the activation, ohmic and concentration losses.

One fuel cell on an average produces $0.7\,V$ and has a current density of $0.8\,\frac{A}{cm^2}$. A fuel cell with area of $100\,cm^2$ hence, can produce around $56\,W$ of power, sufficient
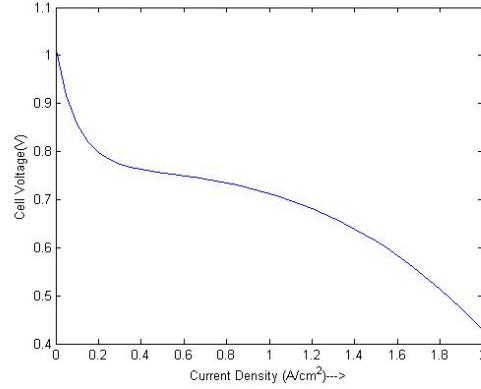
Figure 1.2: V-I Characteristics of PEM Fuel Cell

to power up a single bulb.Since fuel cells are very thin, of the order of $1\,mm$, they are stacked together in series to get higher voltage levels. For example, 100 fuel cells stacked up together can produce approximately $6\,kW$ of power, but will still be only $1\,cm$ thick.

1.2 Literature Review

A lot of research has been done on fuel cell modeling. A simple third order linear model has been proposed in [4, 5]. Third order bi-linear model, US-DoE (US Department of Energy), has been presented in [6]. Then, a third order non-linear model has been shown in [7]. The models of [5, 6, 4, 7] now ignored membrane humidity and pressure of nitrogen in cathode. The model in [8] incorporates these states in a fifth order non-linear model. Finally, an extensive work has been carried out in [9, 10, 11] to develop a fuel cell model for an automobile application. This model is comprehensive and gives a deeper insight into the fuel cell sub-system.

A number of different control strategies have been proposed for the fuel cell. To start with, static and dynamic feedforward controls are developed in [3], followed by LQR feedback control for the 8th order linearized PEM fuel cell model. An H_∞ control features in [12] to achieve robust voltage tracking. Sliding mode control for PEM fuel cell is proposed in [13, 14, 15]. A more comprehensive listing of various control strategies that can be applied to fuel cell can be found in [12].

Chapter 2

Modeling of Fuel Cells

2.1   Fuel Cell System

This work is inspired from the 9th order model developed in [3]. The outline of this chapter is as follows: various fuel cell subsystems are presented first followed by their non-linear equations. This chapter concludes with a summary of all the non-linear equations and corresponding constants.

2.1.1   State Space Model

State space approach is used for modeling the fuel cell. In state space model, each state x represents a physical parameter of the system. In electrical circuits for example, current through inductor or voltage across capacitor represents a state. In mechanical system, displacement,velocity or acceleration of the body represents a state. In the fuel cell model, mass and pressure of various gases are considered to be the states. A non-linear state space model is represented as:

$$\dot{x} = f(x, u) \tag{2.1}$$

Where, x is the state of the system and u is the control input. Following section discusses all the 9 non-linear state equations with derivation.

2.1.2   Fuel Cell Subsystem

Compressor

A static compressor map is used to determine the air flow rate through the compressor. The compressor speed, one of the state variables in the model, is defined using the

concepts of mechanics. The model for the compressor and corresponding non-linear equations are presented below.

The dynamics of the compressor speed ω_{cp} is given by

$$\frac{d\omega_{cp}}{dt} = (\tau_{cm} - \tau_{cp}) \tag{2.2}$$

Where, τ_{cp} [N-m] is the torque required for driving the compressor; τ_{cm} [N-m] is the compressor motor torque.

Further, the torques are given by

$$\tau_{cp} = \frac{C_p}{\omega_{cp}} \frac{T_{atm}}{\eta_{cp}} \left[\left(\frac{p_{sm}}{p_{atm}} \right)^{\frac{\gamma-1}{\gamma}} - 1 \right] W_{cp} \tag{2.3}$$

$$\tau_{cm} = \eta_{cm} \frac{k_t}{R_{cm}} \left(v_{cm} - k_v \omega_{cp} \right) \tag{2.4}$$

C_p is the specific heat capacity of air; γ is ratio of specific heats of air; p_{sm} and p_{atm} are the supply manifold and atmospheric pressures respectively (in atm); k_t, R_{cm} and k_v are motor constants given in Table 2.1.2; η_{cm} is the mechanical efficiency of the motor.

The air temperature at the compressor outlet $T_{cp,out}$ is calculated through

$$T_{cp,out} = T_{atm} + \frac{T_{atm}}{\eta_{cp}} \left[\left(\frac{p_{sm}}{p_{atm}} \right)^{\frac{\gamma-1}{\gamma}} - 1 \right] \tag{2.5}$$

η_{cp} is the maximum efficiency of the compressor.

Compressor air mass flow rate W_{cp} is given by

$$W_{cp} = W_{cr} \frac{\delta}{\sqrt{\theta}} \tag{2.6}$$

Where, W_{cr} is the corrected mass mass flow rate, which takes into account variations in the inlet flow pressure and temperature of the compressor.

$$W_{cr} = \phi \rho_a \frac{\pi}{4} d_c^2 U_c \tag{2.7}$$

ρ_a is the air density [kg/m^3]; d_c is the compressor diameter [m]; U_c is the compressor blade tip speed [m/s]; ϕ is the normalized compressor flow rate.

U_c is determined as follows

$$U_c = \frac{\pi}{60} d_c N_{cr} \tag{2.8}$$

N_{cr} is the corrected compressor speed (in rpm) given by $N_{cr} = N_{cp}/\sqrt{\theta}$ and corrected temperature, $\theta = \frac{T_{cp,in}}{288}$. ϕ is given by the following set of equations

$$\phi = \phi_{max} \left[1 - exp\left(\beta \left(\frac{\psi}{\psi_{max}} - 1 \right) \right) \right]$$ (2.9)

(2.10)

Here, dimensionless head parameter ψ is a given as

$$\psi = C_p T_{cp,in} \left[\left(\frac{p_{cp,out}}{p_{cp,in}} \right)^{\frac{\gamma-1}{\gamma}} \right] / \left(\frac{U_c^2}{2} \right)$$ (2.11)

and, ϕ_{max}, β and ψ_{max} are polynomial function of the Mach number, M given by

$$M = \frac{U_c}{\sqrt{\gamma R_a T_{cp,in}}}$$ (2.12)

$$\phi_{max} = a_4 M^4 + a_3 M^3 + a_2 M^2 + a_1 M + a_0$$ (2.13)

$$\beta = b_2 M^2 + b_1 M + b_0$$ (2.14)

$$\psi_{max} = c_5 M^5 + c_4 M^4 + c_3 M^3 + c_2 M^2 + c_1 M + c_0$$ (2.15)

The regression coefficients a_i, b_i and c_i are given in Table 2.1.2.

The following table lists all the constants required for compressor modeling:

Parameter	Value	Units
$p_{cp,in}$	101325	Pa
$T_{cp,in}$	298.15	K
R_a	2.869×10^2	J/(kg.K)
ρ_a	1.23	kg/m^3
d_c	0.2286	m
δ	1	–
θ	298/288	–

(contd...)

$Parameter$	$Value$	$Units$
a_4	-3.69906×10^{-5}	$-$
a_3	2.70399×10^{-4}	$-$
a_2	-5.36235×10^{-4}	$-$
a_1	-4.63685×10^{-5}	$-$
a_0	2.21195×10^{-3}	$-$
b_2	1.76567	$-$
b_1	-1.34837	$-$
b_0	2.44419	$-$
c_5	-9.78755×10^{-3}	$-$
c_4	0.10581	$-$
c_3	-0.42937	$-$
c_2	0.80121	$-$
c_1	-0.68344	$-$
c_0	0.43331	$-$
J_{cp}	5×10^{-5}	kg.m^2
k_v	0.0153	V/(rad/sec)
k_t	0.0153	N-m/Amp
R_{cm}	0.82	Ω
η_{cm}	98%	$-$

Table 2.1: Compressor Constants

Following figure depicts the Compressor block diagram with all the inputs, outputs and state. Compressor speed, ω_{cp}, is one of the nine state variables of the fuel cell system and is designated x_4
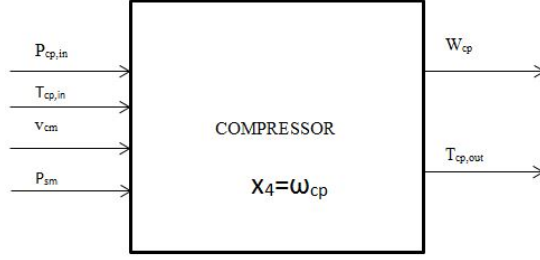
Figure 2.1: Compressor Block

Supply Manifold

The supply manifold is fed by the compressor which in turn feeds air into the cathode. Usually, the air in the supply manifold is not sufficiently humidified and hence needs humidification before being fed into the cathode. The supply manifold pressure and mass are the two state variables of this sub-system. The mass conservation principle is used to determine the mass flow rate through supply manifold and ideal gas equation is used to determine the manifold filling dynamics.

The dynamics of the supply manifold are given by

$$\frac{dm_{sm}}{dt} = W_{cp} - W_{sm,out} \tag{2.16}$$

$$\frac{dp_{sm}}{dt} = \frac{\gamma R_a}{V_{sm}}(W_{cp}T_{cp,out} - W_{sm,out}T_{sm}) \tag{2.17}$$

From the supply manifold perspective, W_{cp} is the inlet mass flow rate from the compressor and $W_{sm,out}$ is the outlet mass flow rate. Further, V_{sm} is the supply manifold volume and T_{sm} is the supply manifold air temperature.

The outlet mass flow rate is calculated using a linearized nozzle flow equation

$$W_{sm,out} = k_{sm,out}(p_{sm} - p_{ca}) \tag{2.18}$$

$k_{sm,out}$ is the supply manifold outlet flow constant and p_{ca} is the cathode pressure.

$Parameter$	$Value$	$Units$
V_{sm}	0.02	m^3
$k_{sm,out}$	0.3629×10^{-5}	kg/(s.Pa)

Table 2.2: Supply Manifold Constants

The two states associated with supply manifold, the pressure, p_{sm} and mass of gas m_{sm} are designated as states x_5 and x_6 respectively.
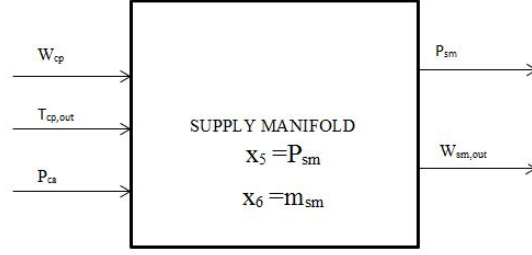
Figure 2.2: Supply Manifold

Cathode

This model computes the mass flow rates of various gases in the cathode. The input for the cathode is humidified air from the compressor. Ideal gas equations and mass-conservation principles are used to obtain differential equations for the states: mass of oxygen, nitrogen, water vapor inside the cathode.

The three state dynamics corresponding to the cathode subsystem are

$$\frac{dm_{O_2,ca}}{dt} = W_{O2,ca,in} - W_{O2,ca,out} - W_{O2,reacted} \tag{2.19}$$

$$\frac{dm_{N_2,ca}}{dt} = W_{N2,ca,in} - W_{O2,reacted} \tag{2.20}$$

$$\frac{dm_{w,ca}}{dt} = W_{v,ca,in} - W_{v,ca,out} + W_{v,ca,gen} + W_{v,membr} \tag{2.21}$$

$W_{O_2,ca,in}$ is the oxygen inlet mass flow rate; $W_{O_2,ca,out}$ is the oxygen outlet mass flow rate; $W_{O_2,reacted}$ is the rate of oxygen reacted; $W_{v,membr}$ is the water flow rate across the fuel cell membrane.

The same notation has been extended for N_2 and H_2O_{ca}.

The partial pressures of oxygen, nitrogen, and the water vapor inside the cathode are calculated using ideal gas law

$$\text{Oxygen gas partial pressure: } p_{O_2,ca} = \frac{m_{O_2,ca}R_{O_2}T_{st}}{V_{ca}} \tag{2.22}$$

$$\text{Nitrogen gas partial pressure: } p_{N_2,ca} = \frac{m_{N_2,ca}R_{N_2}T_{st}}{V_{ca}} \tag{2.23}$$

$$\text{Vapor partial pressure: } p_{v,ca} = \frac{m_{v,ca}R_vT_{st}}{V_{ca}} \tag{2.24}$$

Here, T_{st} is the stack temperature assumed to be constant at $353\,\mathrm{K}$; V_{ca} is the cathode volume; R_{O_2}, R_{N_2} and R_v are gas constants of oxygen, nitrogen and water vapor respectively.

The partial pressure of dry air is

$$p_{a,ca} = p_{O_2,ca} + p_{N_2,ca} \tag{2.25}$$

Total cathode pressure is given by

$$p_{ca} = p_{a,ca} + p_{v,ca} \tag{2.26}$$

The oxygen mole fraction is defined as

$$y_{O_2,ca} = \frac{p_{O_2,ca}}{p_{a,ca}} \tag{2.27}$$

and, relative humidity is given by

$$\phi_{ca} = \frac{p_{v,ca}}{p_{sat}(T_{st})} \tag{2.28}$$

where, $p_{sat}(T_{st})$ is the vapor saturation pressure as a function of the stack temperature T_{st}.

Inlet gas vapor partial pressure can be determined as

$$p_{v,ca,in} = \phi_{ca,in} p_{sat}(T_{ca,in}) \tag{2.29}$$

Partial pressure of inlet dry air can be obtained

$$p_{a,ca,in} = p_{ca,in} - p_{v,ca,in} \tag{2.30}$$

where, $p_{ca,in}$ is the total inlet pressure at cathode

The humidity ratio is

$$\omega_{ca,in} = \frac{M_v}{M_{a,ca,in}} \frac{p_{v,ca,in}}{p_{a,ca,in}} \tag{2.31}$$

The, air molar mass is given by

$$M_{a,ca,in} = y_{O_2,ca,in} M_{O_2} + (1 - y_{O_2,ca,in}) M_{N_2} \tag{2.32}$$

where, M_{O_2} and M_{N_2} are the molar masses of oxygen and nitrogen respectively. $y_{O_2,ca,in}$ is assumed a constant $= 0.21$.

With all the above data, we can now calculate various inlet flows as follows

Mass flow rate of dry air,

$$W_{a,ca,in} = \frac{1}{1 + \omega_{ca,in}} W_{ca,in} \tag{2.33}$$

Mass flow rate of vapor entering cathode,

$$W_{v,ca,in} = W_{ca,in} - W_{a,ca,in} \tag{2.34}$$

Mass flow rate of oxygen,

$$W_{O_2,ca,in} = x_{O_2,ca,in} W_{a,ca,in} \tag{2.35}$$

Mass flow rate of nitrogen,

$$W_{N_2,ca,in} = (1 - x_{O_2,ca,in}) W_{a,ca,in} \tag{2.36}$$

$x_{O_2,ca,in}$ is the oxygen mass fraction defined by

$$x_{O_2,ca,in} = \frac{y_{O_2,ca,in} M_{O_2}}{y_{O_2,ca,in} M_{O_2} + (1 - y_{O2,ca,in}) M_{N_2}} \tag{2.37}$$

The total mass flow rate at the cathode exit is given by a linearized nozzle equation

$$W_{ca,out} = k_{ca,out}(p_{ca} - p_{rm}) \tag{2.38}$$

where, P_{ca} is the cathode pressure, p_{rm} is the return manifold pressure, and $k_{ca,out}$ is the orifice constant. From the knowledge of $W_{ca,out}$ we can determine outlet flow rates of oxygen, nitrogen and vapor following the exact same steps as was done in equations

(2.29) to (2.37)

$$M_{a,ca} = y_{O_2,ca}M_{O_2} + (1 - y_{O_2,ca})M_{N_2} \tag{2.39}$$

$$\omega_{ca,out} = \frac{M_v}{M_{a,ca}}\frac{p_{v,ca}}{p_{a,ca}} \tag{2.40}$$

$$W_{a,ca,out} = \frac{1}{1 + \omega_{ca,out}}W_{ca,out} \tag{2.41}$$

$$W_{v,ca,out} = W_{ca,out} - W_{a,ca,out} \tag{2.42}$$

$$x_{O_2,ca} = \frac{y_{O_2,ca}M_{O_2}}{y_{O_2}M_{O_2} + (1 - y_{O_2,ca})M_{N_2}} \tag{2.43}$$

$$W_{O_2,ca,out} = x_{O_2,ca}W_{a,ca,out} \tag{2.44}$$

$$W_{N_2,ca,out} = (1 - x_{O_2,ca})W_{a,ca,out} \tag{2.45}$$

Using the principles of electrochemistry mass flow rates of oxygen reacted and vapor generated can be calculated as

$$W_{O2,reacted} = M_{O2} \times \frac{nI_{st}}{4F} \tag{2.46}$$

$$W_{v,ca,gen} = M_v \times \frac{nI_{st}}{2F} \tag{2.47}$$

Here, I_{st} is the stack current.

Cathode inlet flow $W_{ca,in}$ is the composition of the dry air from the compressor and water vapor from the humidifier. $W_{ca,in}$ and cathode inlet pressure $p_{ca,in}$ are calculated using a static humidifier model as follows

$$W_{ca,in} = W_{sm,out} + W_{v,inj} \tag{2.48}$$

$$p_{ca,in} = p_{a,cl} + \phi^{des}p_{sat}(T_{cl}) \tag{2.49}$$

$W_{v,inj}$ is the rate of vapor injected and is given by

$$W_{v,inj} = \frac{M_v}{M_a}\frac{\phi^{des}p_{sat}(T_{cl})}{p_{a,cl}}W_{a,cl} - W_{v,cl} \tag{2.50}$$

M_v and M_a are the molar mass of vapor and dry air respectively, ϕ^{des} is the desired inlet humidity, $p_{sat}(T_{cl})$ is the saturation pressure at $T_{cl} = 353\,\text{K}$. The dry air mass flow rate $W_{a,cl}$ and vapor mass flow rate $W_{v,cl}$ is computed as

$$W_{a,cl} = \frac{1}{1 + \omega_{cl}}W_{sm,out} \tag{2.51}$$

$$W_{v,cl} = W_{sm,out} - W_{a,cl} \tag{2.52}$$

Where ω_{cl} is the humidity ratio given by

$$\omega_{cl} = \frac{M_v}{M_a}\frac{p_{v,cl}}{p_{a,cl}} \qquad (2.53)$$

The dry air pressure $p_{a,cl}$ is given as

$$p_{v,cl} = \phi_{cl}p_{sat}(T_{cl}) \qquad (2.54)$$

$$p_{a,cl} = p_{sm} - p_{v,cl} \qquad (2.55)$$

p_{sm}, the supply manifold pressure was defined in (2.17)

$Parameter$	$Value$	$Units$
V_{ca}	0.01	m^3
$k_{ca,out}$	0.2177×10^{-5}	kg/(s.Pa)
$y_{O_2,ca,in}$	0.21	–
$T_{ca,in}$	353	K

Table 2.3: Cathode Constants

The cathode states, x_1,x_3 and x_8 correspond to mass of oxygen, nitrogen and water vapor respectively.
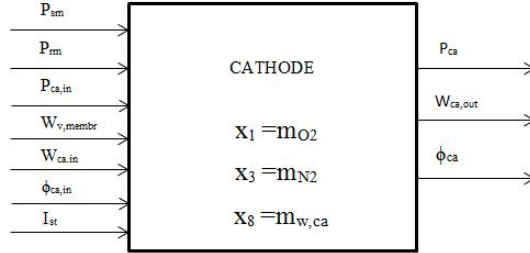

Figure 2.3: Cathode Model

Return Manifold

The return manifold releases un-reacted or partially reacted gases to the atmosphere. The return manifold pressure is the only state variable of this model. Ideal gas law at isothermic conditions is used to determine filling dynamics as follows

$$\frac{dp_{rm}}{dt} = \frac{R_a T_{rm}}{V_{rm}}(W_{ca,out} - W_{rm,out}) \qquad (2.56)$$

Here, it is assumed that changes in air temperature inside return manifold are negligibly small. V_{rm} is the return manifold volume and T_{rm} is the temperature of the gas inside the manifold. $W_{ca,out}$ is cathode outlet flow, as discussed in equation (2.38). The outlet mass flow of return manifold $W_{rm,out}$ is determined using nozzle equations.

$$W_{rm,out} = \frac{C_{D,rm}A_{T,rm}p_{rm}}{\sqrt{RT_{rm}}} \left(\frac{p_{atm}}{p_{rm}}\right)^{\frac{1}{\gamma}} \left\{\frac{2\gamma}{\gamma-1}\left[1-\left(\frac{p_{atm}}{p_{rm}}\right)^{\frac{\gamma-1}{\gamma}}\right]\right\}^{\frac{1}{2}} \tag{2.57}$$

Where, $A_{T,rm}$ is the throttle opening area in m^2; $C_{D,rm}$ is the discharge coefficient of the nozzle; $\bar{R}$ is the universal gas constant.

Parameter	Value	Units
V_{rm}	0.005	m^3
T_{rm}	353	K
$C_{D,rm}$	0.0124	−
$A_{T,rm}$	0.002	m^2

Table 2.4: Return Manifold Constants

The return manifold with it's state x_9 = return manifold pressure is shown below.
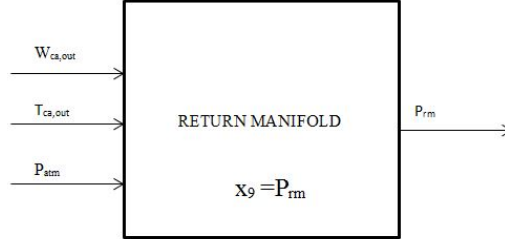

Figure 2.4: Return Manifold

Anode

Anode is fed with hydrogen from a tank. The states for this model are the hydrogen mass inside anode m_{H_2} and water vapor mass $m_{w,an}$. The dynamic equations are

$$\frac{dm_{H_2,an}}{dt} = W_{H_2,an,in} - W_{H_2,reacted} \tag{2.58}$$

$$\frac{dm_{w,an}}{dt} = W_{v,an,in} - W_{v,an,out} - W_{v,membr} \tag{2.59}$$

where, $W_{H_2,an,in}$ is the inlet hydrogen mass flow rate; $W_{H_2,reacted}$ is the rate of hydrogen reacted inside anode; $W_{v,membr}$ is mass flow rate of water transfer across the membrane.

In this work, it is assumed that all outlet flow rates from anode are zero. Similar principles discussed for cathode can be applied to anode to determine various supporting values and parameters.

The partial pressures are,

Hydrogen Gas Partial Pressure:

$$p_{H_2,an} = \frac{m_{H_2,an}R_{H_2}T_{st}}{V_{an}} \tag{2.60}$$

Water Vapor Partial Pressure:

$$p_{v,an} = \frac{m_{v,an}R_vT_{st}}{V_{an}} \tag{2.61}$$

Total Anode Pressure:

$$p_{an} = p_{H_2,an} + p_{v,an} \tag{2.62}$$

Relative humidity of the gas inside anode is

$$\phi_{an} = \frac{p_{v,an}}{p_{sat}(T_{st})} \tag{2.63}$$

$p_{sat}(T_{st})$ is the saturation pressure as a function of stack temperature.

Inlet vapor pressure $p_{v,an,in}$ and inlet hydrogen partial pressure $p_{H_2,an,in}$ are given by

$$p_{v,an,in} = \phi_{an,in}p_{sat}(T_{an,in}) \tag{2.64}$$

$$p_{H_2,an,in} = p_{an,in} - p_{v,an,in} \tag{2.65}$$

Now, we find the anode humidity ratio as

$$\omega_{an,in} = \frac{M_v}{M_{H_2}}\frac{p_{v,an,in}}{p_{a,an,in}} \tag{2.66}$$

Here, M_v is the molar mass of vapor and M_{H_2} is the molar mass of the hydrogen gas.

Finally, with all the above data, we can find various inlet flow rates as

$$W_{H_2,an,in} = \frac{1}{1 + \omega_{an,in}}W_{an,in} \tag{2.67}$$

$$W_{v,an,in} = W_{an,in} - W_{H_2,an,in} \tag{2.68}$$

Where, the anode inlet flow $W_{an,in}$ is given by

$$W_{an,in} = K_1(K_2 p_{sm} - p_{an}) \tag{2.69}$$

$W_{an,in}$ is assumed to be controlled by a simple proportional control that minimizes the pressure difference across the membrane. Since cathode pressure cannot be measured directly, it's approximate value equal to $K_2 p_{sm}$ is used in the equation. Here, K_2 takes into account the pressure drop between the supply manifold and cathode and K_1 is the gain of the proportional controller.

The rate of hydrogen reacted or consumed during the electrochemical reaction is given by

$$W_{H_2,reacted} = M_{H_2} \times \frac{nI_{st}}{2F} \tag{2.70}$$

$Parameter$	$Value$	$Units$
V_{an}	0.005	kg/m^3
$T_{an,in}$	353	K
$\phi_{an,in}$	1	$-$

Table 2.5: Anode Constants

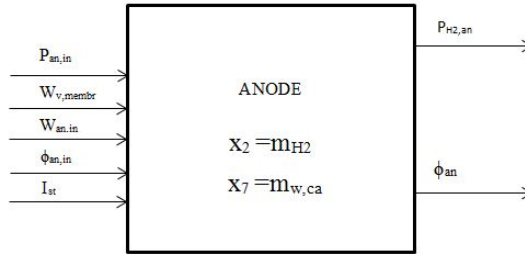The anode block diagram and its corresponding designated states are presented below

Figure 2.5: Anode Model

Membrane Hydration

This model captures the dynamics associated with water mass flow rate across the membrane. The mass flow rate obtained in this model is used in both the cathode and anode model.

The water flow across the membrane is given by

$$N_{v,membr} = n_d \frac{i}{F} - D_w \frac{c_{v,ca} - c_{v,an}}{t_m} \tag{2.71}$$

Where, t_m is the membrane thickness [cm]; n_d is the electro-osmotic drag coefficient; D_w is diffusion coefficient [cm^2/sec]; c_v is the water concentration [mol/cm^3].

Each of the above constants are presented below.

Water concentration at the membrane surface is given by

$$c_{v,an} = \frac{\rho_{m,dry}}{M_{m,dry}} \lambda_{an} \tag{2.72}$$

$$c_{v,ca} = \frac{\rho_{m,dry}}{M_{m,dry}} \lambda_{ca} \tag{2.73}$$

Where, $\rho_{m,dry}$ is the membrane dry density in kg/cm^3 and $M_{m,dry}$ is the membrane dry equivalent weight in kg/mol. The water content in the membrane, λ_i is defined as

$$\lambda_i = \begin{cases} 0.043 + 17.81a_i - 39.85a_i^2 + 36.0a_i^3, & 0 < a_i < 1. \\ 14 + 1.4(a_i - 1), & 1 < a_i \le 3. \end{cases} \tag{2.74}$$

Where, a_i is the water activity and the subscript i denotes either anode (an), cathode (ca) or membrane (m). These activities are defined below

$$a_i = \frac{p_{v,i}}{p_{sat,i}} \tag{2.75}$$

$$a_m = \frac{a_{an} + a_{ca}}{2} \tag{2.76}$$

Electro-osmotic drag coefficient can be determined from the membrane water content λ_m as

$$n_d = 0.0029\lambda_m^2 + 0.05\lambda_m - 3.4 \times 10^{-19} \tag{2.77}$$

The diffusion coefficient is given by

$$D_w = D_\lambda \exp\left(2416\left(\frac{1}{303} - \frac{1}{T_{fc}}\right)\right) \tag{2.78}$$

Where D_λ is assumed to be a constant equal to 1.25×10^{-6} and T_{fc} is the fuel cell temperature, assumed to be equal to the stack temperature. $N_{v,membr}$ [mol/(sec.cm^2)]

gives the water flow rate per unit area in one fuel cell. The total mass flow rate across the entire fuel cell stack is given by

$$W_{v,membr} = N_{v,membr} \times M_v \times A_{fc} \times 10^4 \times n \tag{2.79}$$

M_v is the molar mass of vapor, A_{fc} is the fuel cell area in cm^2 and n is the number of fuel cells in the stack.

$Parameter$	$Value$	$Units$
$\rho_{m,dry}$	0.002	kg/cm^3
$M_{m,dry}$	1.1	kg/mol
t_m	0.01275×10^{-2}	m
A_{fc}	280×10^{-4}	m^2
D_λ	1.25×10^{-6}	–
λ_m	14	–

Table 2.6: Membrane Hydration Constants

The membrane hydration model generates constants for the rest of the subsystem and hence has no states associated with it. The following block diagram shows the input and output of the membrane hydration model.
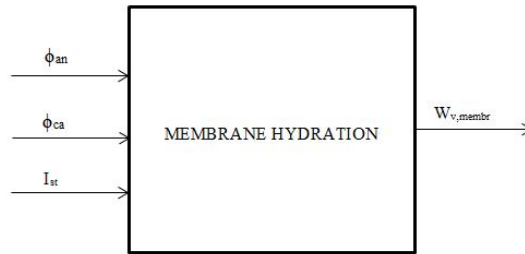
Figure 2.6: Membrane Hydration Model

2.1.3 Non Linear Equations

In this section, all the nine non-linear equations of the PEM fuel cell are presented. These equations are derived from the discussion of various subsystems, presented previously. They are represented using state space form with

$$x_1 = \text{Mass of oxygen in cathode}$$

$$x_2 = \text{Mass of hydrogen in anode}$$

$$x_3 = \text{Mass of nitrogen in cathode}$$

$$x_4 = \text{Compressor angular speed}$$

$$x_5 = \text{Supply manifold pressure}$$

$$x_6 = \text{Mass of gas in supply manifold}$$

$$x_7 = \text{Mass of water in anode}$$

$$x_8 = \text{Mass of water in cathode}$$

$$x_9 = \text{Return manifold pressure}$$

All masses are expressed in grams, pressures are in bar and the compressor speed is in rad/s.

$$\dot{x}_1 = \frac{M_{O_2}\, yO_{2,ca,in}}{\left(M_{O_2}\, yO_{2,ca,in} - M_{N_2}\left(yO_{2,ca,in}-1\right)\right)}$$

$$* \left[\frac{k_{sm,out}\left(x_5 - \dfrac{t_{st}\left(R_{O_2}x_1+R_{N_2}x_3+R_v x_8\right)}{V_{ca}}\right)}{\dfrac{M_v\,p_{sat}(T_{atm})\phi_{atm}x_5}{M_a\,P_{atm}\left(x_5-\frac{p_{sat}(T_{atm})\phi_{atm}x_5}{P_{atm}}\right)}+1} + \frac{M_v\,k_{sm,out}\,p_{sat}(T_{cl})\,\phi^{des}\left(x_5 - \dfrac{t_{st}\left(R_{O_2}x_1+R_{N_2}x_3+R_v x_8\right)}{V_{ca}}\right)}{M_a\left(x_5-\dfrac{p_{sat}(T_{atm})\phi_{atm}x_5}{P_{atm}}\right)\left(\dfrac{M_v\,p_{sat}(T_{atm})\phi_{atm}x_5}{P_{atm}}+1\right)} \right]$$

$$* \left[\frac{M_v\,p_{sat}(T_{atm})\,p_{sat}(T_{ca,in})\,x_5}{2\,P_{atm}\,p_{sat}(T_{cl})\left(M_{O_2}\,yO_{2,ca,in}-M_{N_2}\left(yO_{2,ca,in}-1\right)\right)\left(x_5+p_{sat}(T_{cl})\,\phi^{des}-\dfrac{p_{sat}(T_{atm})\phi_{atm}x_5}{P_{atm}}-\dfrac{p_{sat}(T_{atm})\,p_{sat}(T_{ca,in})\,x_5}{2\,P_{atm}\,p_{sat}(T_{cl})}\right)}+1 \right]$$

$$- \frac{M_{O_2}\,i_{st}\,n}{4F}$$

$$+ M_{O_2}\,R_{O_2}\,k_{ca,out}\,t_{st}\,x_1\left(x_9 - \frac{t_{st}\left(R_{O_2}x_1+R_{N_2}x_3+R_v x_8\right)}{V_{ca}}\right)$$

$$* \left[\frac{M_v\,R_v\,t_{st}\,x_8}{V_{ca}\left(\dfrac{R_{O_2}t_{st}x_1}{V_{ca}\left(\frac{R_{O_2}t_{st}x_1}{V_{ca}}+\frac{R_{N_2}t_{st}x_3}{V_{ca}}\right)}-1\right)\left(M_{N_2}\left(\dfrac{R_{O_2}t_{st}x_1}{V_{ca}\left(\frac{R_{O_2}t_{st}x_1}{V_{ca}}+\frac{R_{N_2}t_{st}x_3}{V_{ca}}\right)}-1\right)-\dfrac{M_{O_2}R_{O_2}t_{st}x_1}{V_{ca}\left(\frac{R_{O_2}t_{st}x_1}{V_{ca}}+\frac{R_{N_2}t_{st}x_3}{V_{ca}}\right)}\right)} \right.$$

$$\left. \frac{1}{\left(\dfrac{R_{O_2}t_{st}x_1}{V_{ca}\left(\frac{R_{O_2}t_{st}x_1}{V_{ca}}+\frac{R_{N_2}t_{st}x_3}{V_{ca}}\right)}-1\right)-\dfrac{M_{O_2}R_{O_2}t_{st}x_1}{V_{ca}\left(\frac{R_{O_2}t_{st}x_1}{V_{ca}}+\frac{R_{N_2}t_{st}x_3}{V_{ca}}\right)}} \right]$$

$$* \left[M_{N_2}\left(\dfrac{R_{O_2}t_{st}x_1}{V_{ca}\left(\frac{R_{O_2}t_{st}x_1}{V_{ca}}+\frac{R_{N_2}t_{st}x_3}{V_{ca}}\right)}-1\right)\left(\frac{R_{O_2}t_{st}x_1}{V_{ca}}+\frac{R_{N_2}t_{st}x_3}{V_{ca}}\right) \right]$$

$$\tag{2.80}$$

$$\dot{x}_2 = \frac{K_1\left(K_2\, x_5 - \dfrac{t_{st}\left(R_{H_2}\, x_2 + R_v\, x_7\right)}{V_{an}}\right)}{\dfrac{M_v\, p_{sat}(T_{an,in})\,\phi_{an,in}}{M_{H_2}\, p_{an,in}} + 1} - \frac{M_{H_2}\, i_{st}\, n}{2F} \tag{2.81}$$

$$\dot{x}_3 = -\left(\frac{M_{O_2}\, yO_{2,ca,in}}{M_{O_2}\, yO_{2,ca,in} - M_{N_2}\left(yO_{2,ca,in} - 1\right)} - 1\right)$$

$$* \frac{\dfrac{k_{sm,out}\left(x_5 - \dfrac{t_{st}\left(R_{O_2}\, x_1 + R_{N_2}\, x_3 + R_v\, x_8\right)}{V_{ca}}\right)}{\dfrac{M_v\, p_{sat}(T_{atm})\,\phi_{atm}\, x_5}{M_a\, P_{atm}\left(x_5 - \dfrac{p_{sat}(T_{atm})\,\phi_{atm}\, x_5}{P_{atm}}\right)} + 1} + \dfrac{M_v\, k_{sm,out}\, p_{sat}(T_{cl})\,\phi^{des}\left(x_5 - \dfrac{t_{st}\left(R_{O_2}\, x_1 + R_{N_2}\, x_3 + R_v\, x_8\right)}{V_{ca}}\right)}{M_a\left(x_5 - \dfrac{p_{sat}(T_{atm})\,\phi_{atm}\, x_5}{P_{atm}}\right)\left(\dfrac{M_v\, p_{sat}(T_{atm})\,\phi_{atm}\, x_5}{M_a\, P_{atm}\left(x_5 - \dfrac{p_{sat}(T_{atm})\,\phi_{atm}\, x_5}{P_{atm}}\right)} + 1\right)}}{\dfrac{M_v\, p_{sat}(T_{atm})\, p_{sat}(T_{ca,in})\, x_5}{2\, P_{atm}\, p_{sat}(T_{cl})\left(M_{O_2}\, yO_{2,ca,in} - M_{N_2}\left(yO_{2,ca,in} - 1\right)\right)\left(x_5 + p_{sat}(T_{atm})\,\phi_{atm}\, x_5 - \dfrac{p_{sat}(T_{atm})\, p_{sat}(T_{ca,in})\, x_5}{2\, P_{atm}\, p_{sat}(T_{cl})}\right)} + 1}$$

$$- \left(x_9 - \frac{t_{st}\left(R_{O_2}\, x_1 + R_{N_2}\, x_3 + R_v\, x_8\right)}{V_{ca}}\right)$$

$$* \frac{k_{ca,out}\dfrac{M_{O_2}\, R_{O_2}\, t_{st}\, x_1}{\dfrac{R_{O_2}\, t_{st}\, x_1}{V_{ca}\left(\dfrac{R_{O_2}\, t_{st}\, x_1}{V_{ca}} + \dfrac{R_{N_2}\, t_{st}\, x_3}{V_{ca}}\right)}}\left(M_{N_2}\left(\dfrac{\dfrac{R_{O_2}\, t_{st}\, x_1}{V_{ca}}}{V_{ca}\left(\dfrac{R_{O_2}\, t_{st}\, x_1}{V_{ca}} + \dfrac{R_{N_2}\, t_{st}\, x_3}{V_{ca}}\right)} - 1\right) - \dfrac{M_{O_2}\, R_{O_2}\, t_{st}\, x_1}{V_{ca}\left(\dfrac{R_{O_2}\, t_{st}\, x_1}{V_{ca}} + \dfrac{R_{N_2}\, t_{st}\, x_3}{V_{ca}}\right)}\right) + 1}{M_v\, R_v\, t_{st}\, x_8\left(\dfrac{\dfrac{R_{O_2}\, t_{st}\, x_1}{V_{ca}}}{V_{ca}\left(\dfrac{R_{O_2}\, t_{st}\, x_1}{V_{ca}} + \dfrac{R_{N_2}\, t_{st}\, x_3}{V_{ca}}\right)} - 1\right)M_{N_2} - \dfrac{M_{O_2}\, R_{O_2}\, t_{st}\, x_1}{V_{ca}\left(\dfrac{R_{O_2}\, t_{st}\, x_1}{V_{ca}} + \dfrac{R_{N_2}\, t_{st}\, x_3}{V_{ca}}\right)} - 1} \tag{2.82}$$

$$
\begin{aligned}
\dot{x}_4 =\; & \frac{\dfrac{\eta_{cm}\,k_t\,(u-k_v\,x_4)}{\eta_{cp}}}{J_{cp}} + \frac{\pi\,C_p\,d_c{}^3\,\rho_a\,\delta\,T_{atm}\left(\left(\dfrac{x_5}{P_{atm}}\right)^{\frac{\gamma-1}{\gamma}}-1\right)}{8\,\eta_{cm}\,\theta\,J_{cp}} \\[2em]
& *\; e^{\left(\dfrac{d_c{}^2\,x_4{}^2\left(c_0+\dfrac{c_3\,d_c{}^3\,x_4{}^3}{8\,\theta^{\frac{3}{2}}\,(R_a\,\gamma\,T_{atm})^{\frac{3}{2}}}+\dfrac{c_5\,d_c{}^5\,x_4{}^5}{32\,\theta^{\frac{5}{2}}\,(R_a\,\gamma\,T_{atm})^{\frac{5}{2}}}+\dfrac{c_1\,d_c\,x_4}{2\sqrt{\theta}\sqrt{R_a\,\gamma\,T_{atm}}}+\dfrac{c_2\,d_c{}^2\,x_4{}^2}{4\,R_a\,\gamma\,T_{atm}\,\theta}+\dfrac{c_4\,d_c{}^4\,x_4{}^4}{16\,R_a{}^2\,\gamma^2\,T_{atm}{}^2\,\theta^2}\right)}{8\,c_p\,T_{atm}\,\theta\left(\left(\dfrac{x_5}{P_{atm}}\right)^{\frac{\gamma-1}{\gamma}}-1\right)}\right)^{-1}} \\[2em]
& *\left(a_0+\frac{a_3\,d_c{}^3\,x_4{}^3}{8\,\theta^{\frac{3}{2}}\,(R_a\,\gamma\,T_{atm})^{\frac{3}{2}}}+\frac{a_1\,d_c\,x_4}{2\sqrt{\theta}\sqrt{R_a\,\gamma\,T_{atm}}}+\frac{a_2\,d_c{}^2\,x_4{}^2}{4\,R_a\,\gamma\,T_{atm}\,\theta}+\frac{a_4\,d_c{}^4\,x_4{}^4}{16\,R_a{}^2\,\gamma^2\,T_{atm}{}^2\,\theta^2}\right) \\[2em]
& \left(b_0+\frac{b_1\,d_c\,x_4}{2\sqrt{\theta}\sqrt{R_a\,\gamma\,T_{atm}}}+\frac{b_2\,d_c{}^2\,x_4{}^2}{4\,R_a\,\gamma\,T_{atm}\,\theta}\right)^{-1}
\end{aligned}
\tag{2.83}
$$

$$\dot{x}_5 = -\frac{R_a\,\gamma}{V_{sm}}\,\frac{k_{sm,out}\,V_{sm}\,x_5\left(x_5 - \dfrac{t_{st}\left(R_{O_2}\,x_1 + R_{N_2}\,x_3 + R_v\,x_8\right)}{V_{ca}}\right)}{R_a\,x_6}$$

$$-\frac{R_a\,\gamma}{V_{sm}}\,\frac{\pi\,d_c^{\,3}\,\rho_a\,\delta\,x_4}{8\,\theta}$$

$$* \left(e^{\dfrac{d_c^{\,2} x_4^{\,2}\left(c_0 + \dfrac{c_3\,d_c^{\,3}\,x_4^{\,3}}{8\,\theta^{\frac{3}{2}}\left(R_a\,\gamma\,T_{atm}\right)^{\frac{3}{2}}} + \dfrac{c_5\,d_c^{\,5}\,x_4^{\,5}}{32\,\theta^{\frac{5}{2}}\left(R_a\,\gamma\,T_{atm}\right)^{\frac{5}{2}}} + \dfrac{c_1\,d_c\,x_4}{2\sqrt{\theta}\sqrt{R_a\,\gamma\,T_{atm}}} + \dfrac{c_2\,d_c^{\,2}\,x_4^{\,2}}{4\,R_a\,\gamma\,T_{atm}\,\theta} + \dfrac{c_4\,d_c^{\,4}\,x_4^{\,4}}{16\,R_a^{\,2}\,\gamma^2\,T_{atm}^{\,2}\,\theta^2}\right)}{8\,c_p\,T_{atm}\,\theta\left(\left(\frac{x_5}{P_{atm}}\right)^{\frac{\gamma-1}{\gamma}} - 1\right)}} - 1 \right)$$

$$\left(b_0 + \frac{b_1\,d_c\,x_4}{2\sqrt{\theta}\sqrt{R_a\,\gamma\,T_{atm}}} + \frac{b_2\,d_c^{\,2}\,x_4^{\,2}}{4\,R_a\,\gamma\,T_{atm}\,\theta}\right)^{-1}$$

$$* \left(T_{atm} + \frac{5\,T_{atm}\left(\left(\frac{x_5}{P_{atm}}\right)^{\frac{\gamma-1}{\gamma}} - 1\right)}{4}\right)$$

$$\left(a_0 + \frac{a_3\,d_c^{\,3}\,x_4^{\,3}}{8\,\theta^{\frac{3}{2}}\left(R_a\,\gamma\,T_{atm}\right)^{\frac{3}{2}}} + \frac{a_1\,d_c\,x_4}{2\sqrt{\theta}\sqrt{R_a\,\gamma\,T_{atm}}} + \frac{a_2\,d_c^{\,2}\,x_4^{\,2}}{4\,R_a\,\gamma\,T_{atm}\,\theta} + \frac{a_4\,d_c^{\,4}\,x_4^{\,4}}{16\,R_a^{\,2}\,\gamma^2\,T_{atm}^{\,2}\,\theta^2}\right)^{-1}$$

$$(2.84)$$

$$\dot{x}_6 = -k_{sm,out}\left(x_5 - \frac{t_{st}\left(R_{O_2}\,x_1 + R_{N_2}\,x_3 + R_v\,x_8\right)}{V_{ca}}\right)$$

$$-\frac{\pi\,d_c{}^3\,\rho_a\,\delta\,x_4}{8\,\theta}$$

$$*\left(e^{\dfrac{d_c{}^2 x_4{}^2\left(c_0 + \frac{c_3\,d_c{}^3 x_4{}^3}{8\,\theta^{\frac{3}{2}}\,(R_a\,\gamma\,T_{atm})^{\frac{3}{2}}} + \frac{c_5\,d_c{}^5 x_4{}^5}{32\,\theta^{\frac{5}{2}}\,(R_a\,\gamma\,T_{atm})^{\frac{5}{2}}} + \frac{c_1\,d_c\,x_4}{2\sqrt{\theta}\,\sqrt{R_a\,\gamma\,T_{atm}}} + \frac{c_2\,d_c{}^2 x_4{}^2}{4\,R_a\,\gamma\,T_{atm}\,\theta} + \frac{c_4\,d_c{}^4 x_4{}^4}{16\,R_a{}^2\,\gamma^2\,T_{atm}{}^2\,\theta^2}\right)}{8\,c_p\,T_{atm}\,\theta}}\left(\left(\frac{x_5}{P_{atm}}\right)^{\frac{\gamma-1}{\gamma}}-1\right)-1\right)^{-1}$$

$$*\left(a_0 + \frac{a_3\,d_c{}^3\,x_4{}^3}{8\,\theta^{\frac{3}{2}}\,(R_a\,\gamma\,T_{atm})^{\frac{3}{2}}} + \frac{a_1\,d_c\,x_4}{2\sqrt{\theta}\,\sqrt{R_a\,\gamma\,T_{atm}}} + \frac{a_2\,d_c{}^2\,x_4{}^2}{4\,R_a\,\gamma\,T_{atm}\,\theta} + \frac{a_4\,d_c{}^4\,x_4{}^4}{16\,R_a{}^2\,\gamma^2\,T_{atm}{}^2\,\theta^2}\right)$$

$$\left(b_0 + \frac{b_1\,d_c\,x_4}{2\sqrt{\theta}\,\sqrt{R_a\,\gamma\,T_{atm}}} + \frac{b_2\,d_c{}^2\,x_4{}^2}{4\,R_a\,\gamma\,T_{atm}\,\theta}\right) - 1 \tag{2.85}$$

$$\dot{x}_7 = K_1\left(K_2\,x_5 - \frac{t_{st}\left(R_{H_2}\,x_2 + R_v\,x_7\right)}{V_{an}}\right) - \frac{K_1\left(K_2\,x_5 - \frac{t_{st}\left(R_{H_2}\,x_2 + R_v\,x_7\right)}{V_{an}}\right)}{\dfrac{M_v\,P_{sat}(T_{an,in})\,\phi_{an,in}}{M_{H_2}\,P_{an,in}} + 1}$$

$$-\,10^4\,A_{fc}\,M_v\,n\left(\frac{D_\lambda\,e^{\frac{2416}{303}-\frac{2416}{t_{st}}}\left(\dfrac{14\,\rho_{m,dry}}{M_{m,dry}} - \dfrac{\rho_{m,dry}\left(\gamma\left(\frac{R\,t_{st}\,x_8}{M_v\,P_{sat}(T_{st})\,V_{an}}-1\right)+14\right)}{M_{m,dry}}\right)}{10^2\,t_m} + \frac{i_{st}\,n_d}{10^8\,A_{fc}\,F}\right) \tag{2.86}$$

$$
\dot{x}_8 = k_{ca,out}\left(x_9 - \frac{t_{st}\left(R_{O_2}\,x_1 + R_{N_2}\,x_3 + R_v\,x_8\right)}{V_{ca}}\right)
$$

$$
- \frac{k_{sm,out}\left(x_5 - \frac{t_{st}\left(R_{O_2}\,x_1 + R_{N_2}\,x_3 + R_v\,x_8\right)}{V_{ca}}\right)}{\frac{M_v\,p_{sat}(T_{atm})\,\phi_{atm}\,x_5}{M_a\,P_{atm}\left(x_5 - \frac{p_{sat}(T_{atm})\,\phi_{atm}\,x_5}{P_{atm}}\right)} + 1}
$$

$$
+ \frac{M_v\,k_{sm,out}\,p_{sat}(T_{cl})\,\phi^{des}\left(x_5 - \frac{t_{st}\left(R_{O_2}\,x_1 + R_{N_2}\,x_3 + R_v\,x_8\right)}{V_{ca}}\right)}{M_a\left(x_5 - \frac{p_{sat}(T_{atm})\,\phi_{atm}\,x_5}{P_{atm}}\right)\left(\frac{M_v\,p_{sat}(T_{atm})\,\phi_{atm}\,x_5}{M_a\,P_{atm}\left(x_5 - \frac{p_{sat}(T_{atm})\,\phi_{atm}\,x_5}{P_{atm}}\right)} + 1\right)}
$$

$$
- \frac{M_v\,p_{sat}(T_{atm})\,p_{sat}(T_{ca,in})\,x_5}{2\,P_{atm}\,p_{sat}(T_{cl})\left(M_{O_2}\,y_{O_2,ca,in} - M_{N_2}\left(y_{O_2,ca,in} - 1\right)\right)\left(x_5 + p_{sat}(T_{cl})\,\phi^{des} - \frac{p_{sat}(T_{atm})\,\phi_{atm}\,x_5}{P_{atm}} - \frac{p_{sat}(T_{atm})\,p_{sat}(T_{ca,in})\,x_5}{2\,P_{atm}\,p_{sat}(T_{cl})}\right)}
$$

$$
+ \frac{k_{sm,out}\left(x_5 - \frac{t_{st}\left(R_{O_2}\,x_1 + R_{N_2}\,x_3 + R_v\,x_8\right)}{V_{ca}}\right)}{\frac{M_v\,p_{sat}(T_{atm})\,\phi_{atm}\,x_5}{M_a\,P_{atm}\left(x_5 - \frac{p_{sat}(T_{atm})\,\phi_{atm}\,x_5}{P_{atm}}\right)} + 1}
$$

$$
+ \frac{k_{ca,out}\left(x_9 - \frac{t_{st}\left(R_{O_2}\,x_1 + R_{N_2}\,x_3 + R_v\,x_8\right)}{V_{ca}}\right)}{M_v\,R_v\,t_{st}\,x_8}\left(M_{N_2}\left(\frac{\frac{R_{O_2}\,t_{st}\,x_1}{V_{ca}}}{V_{ca}\left(\frac{R_{O_2}\,t_{st}\,x_1}{V_{ca}} + \frac{R_{N_2}\,t_{st}\,x_3}{V_{ca}}\right)} - 1\right) - \frac{M_{O_2}\,R_{O_2}\,t_{st}\,x_1}{V_{ca}\left(\frac{R_{O_2}\,t_{st}\,x_1}{V_{ca}} + \frac{R_{N_2}\,t_{st}\,x_3}{V_{ca}}\right)} - 1\right)
$$

$$
+ \frac{M_v\,i_{st}\,n}{2\,F}
$$

$$
+ 10^4\,A_{fc}\,M_v\,n\left(\frac{D_\lambda\,e^{\frac{2416}{303} - \frac{2416}{t_{st}}}\left(\frac{14\,\rho_{m,dry}}{M_{m,dry}} - \frac{\rho_{m,dry}\left(\gamma\left(\frac{R\,t_{st}\,x_8}{M_v\,p_{sat}(T_{st})\,V_{an}} - 1\right) + 14\right)}{M_{m,dry}}\right)}{10^2\,t_m} + \frac{i_{st}\,n_d}{108\,A_{fc}\,F}\right)
$$

$$
+ \frac{M_v\,k_{sm,out}\,p_{sat}(T_{cl})\,\phi^{des}\left(x_5 - \frac{t_{st}\left(R_{O_2}\,x_1 + R_{N_2}\,x_3 + R_v\,x_8\right)}{V_{ca}}\right)}{M_a\left(x_5 - \frac{p_{sat}(T_{atm})\,\phi_{atm}\,x_5}{P_{atm}}\right)\left(\frac{M_v\,p_{sat}(T_{atm})\,\phi_{atm}\,x_5}{M_a\,P_{atm}\left(x_5 - \frac{p_{sat}(T_{atm})\,\phi_{atm}\,x_5}{P_{atm}}\right)} + 1\right)}
$$

$$
\tag{2.87}
$$

$$\dot{x}_9 = \frac{R_a\,T_{rm}\left(k_{ca,out}\left(x_9 - \dfrac{t_{st}\left(R_{O_2}\,x_1 + R_{N_2}\,x_3 + R_v\,x_8\right)}{V_{ca}}\right)\right) + \dfrac{\sqrt{7}\,A_{T,rm}\,C_{D,rm}\,x_9\sqrt{1-\left(\frac{P_{atm}}{x_9}\right)^{\frac{\gamma-1}{\gamma}}}\left(\frac{P_{atm}}{x_9}\right)^{\frac{1}{\gamma}}}{\sqrt{(R)}}}{V_{rm}}$$

$$(2.88)$$

$$y_1 = \frac{\pi\,d_c^{\,3}\,\rho_a\,\delta\,x_4\left(e^{\dfrac{d_c^{\,2}\,x_4^{\,2}\left(c_0 + \frac{c_3\,d_c^{\,3}\,x_4^{\,3}}{8\,\theta^{\frac{3}{2}}\,(R_a\,\gamma\,T_{atm})^{\frac{3}{2}}} + \frac{c_5\,d_c^{\,5}\,x_4^{\,5}}{32\,\theta^{\frac{5}{2}}\,(R_a\,\gamma\,T_{atm})^{\frac{5}{2}}} + \frac{c_1\,d_c\,x_4}{2\sqrt{\theta}\sqrt{R_a\,\gamma\,T_{atm}}} + \frac{c_2\,d_c^{\,2}\,x_4^{\,2}}{4\,R_a\,\gamma\,T_{atm}\,\theta} + \frac{c_4\,d_c^{\,4}\,x_4^{\,4}}{16\,R_a^{\,2}\,\gamma^2\,T_{atm}^{\,2}\,\theta^2}\right)}{8\,c_p\,T_{atm}\,\theta}}\left(\left(\frac{x_5}{p_{atm}}\right)^{\frac{\gamma-1}{\gamma}}-1\right)-1\right)\left(b_0 + \frac{b_1\,d_c\,x_4}{2\sqrt{\theta}\sqrt{R_a\,\gamma\,T_{atm}}} + \frac{b_2\,d_c^{\,2}\,x_4^{\,2}}{4\,R_a\,\gamma\,T_{atm}\,\theta}\right)}{8\,\theta}$$

$$*\left(a_0 + \frac{a_3\,d_c^{\,3}\,x_4^{\,3}}{8\,\theta^{\frac{3}{2}}\,(R_a\,\gamma\,T_{atm})^{\frac{3}{2}}} + \frac{a_1\,d_c\,x_4}{2\sqrt{\theta}\sqrt{R_a\,\gamma\,T_{atm}}} + \frac{a_2\,d_c^{\,2}\,x_4^{\,2}}{4\,R_a\,\gamma\,T_{atm}\,\theta} + \frac{a_4\,d_c^{\,4}\,x_4^{\,4}}{16\,R_a^{\,2}\,\gamma^2\,T_{atm}^{\,2}\,\theta^2}\right)$$

$$(2.89)$$

$$y_2 = x_5$$

$$(2.90)$$

$$
\begin{aligned}
y_3 = {} & -n\left(\left(\left(e^{-\frac{c_1\,i_{st}}{10^4 A_{fc}}} - 1\right)\left(\frac{29\,t_{fc}}{5\times10^4} - \frac{83}{500}\right)\left(\frac{p_{sat}}{10^5} + \frac{R_{O_2}\,t_{st}\,\mathrm{x}_1}{1.173\times10^4\,v_{ca}}\right)\right)\right) \\
& -n\left(\left(\left(\frac{4.775\times10^{15}\,t_{fc}}{2.951\times10^{20}} - \frac{809}{50000}\right)\left(\frac{p_{sat}}{10^5} + \frac{R_{O_2}\,t_{st}\,\mathrm{x}_1}{1.173\times10^4\,v_{ca}}\right)^2 - \frac{717}{1250}\right)\right) \\
& -n\left(\frac{\ln\left(-\frac{\frac{1173\,p_{sat}}{10^5} - \frac{1173\,t_{st}\left(R_{O_2}\,\mathrm{x}_1 + R_{N_2}\,\mathrm{x}_3 + R_v\,\mathrm{x}_8\right)}{10^5\,v_{ca}}}{p_{atm}}\right)}{2} + \ln\left(-\frac{p_{sat} - \frac{t_{st}\left(R_{O_2}\,\mathrm{x}_1 + R_{N_2}\,\mathrm{x}_3 + R_v\,\mathrm{x}_8\right)}{v_{ca}}}{p_{atm}}\right)}{\frac{6.358\times10^{15}\,t_{fc}}{1.475\times10^{20}}}\right) \\
& +n\left(\frac{\ln\left(\frac{R_{O_2}\,t_{st}\,\mathrm{x}_1}{p_{atm}\,v_{ca}}\right)}{2} + \ln\left(\frac{R_h\,2\,t_{st}\,\mathrm{x}_2}{p_{atm}\,v_{an}}\right)}{\frac{6.357\times10^{15}\,t_{fc}}{1.475\times10^{20}}}\right) \\
& +n\left(\frac{i_{st}\,\mathrm{t_m}\,e^{\mathrm{b}2\left(\frac{1}{t_{fc}} - \frac{1}{303}\right)}}{100\,A_{fc}\,\mathrm{b}_1} - \frac{19}{20}\right) \\
& + \frac{i_{st}\left(\frac{i_{st}\left(\left(\frac{1.597\times10^{15}\,t_{fc}}{1.844\times10^{19}} - \frac{17}{250}\right)\left(\frac{p_{sat}}{10^5} + \frac{R_{O_2}\,t_{st}\,\mathrm{x}_1}{1.173\times10^4\,v_{ca}}\right) - \frac{t_{fc}}{6250} + \frac{27}{50}\right)}{\left(10^5\,A_{fc}\,i_{max}\right)}\right)^{\mathrm{c}3}}{10^5\,A_{fc}}
\end{aligned}
$$

(2.91)

Chapter 3

Simulation of the Fuel Cell Model

3.1 SIMULINK implementation of Subsystems

In this section, the SIMULINK models of the fuel cell subsystems are presented. Various subsystem blocks are individually discussed and all the subsystem blocks are finally inter-connected to form an entire PEM fuel cell. The blocks are implementation of the non-linear equations discussed in Chapter 2.

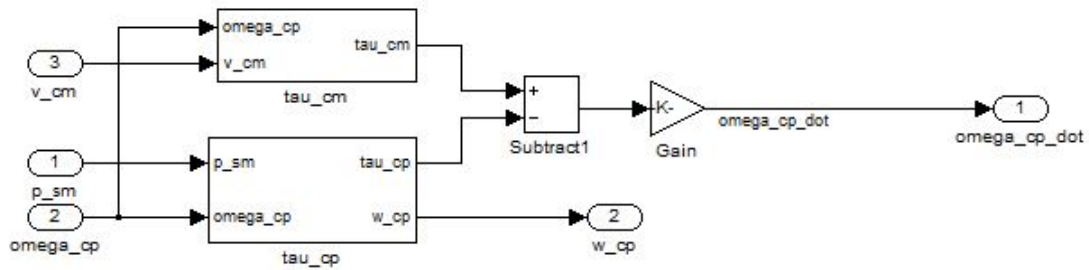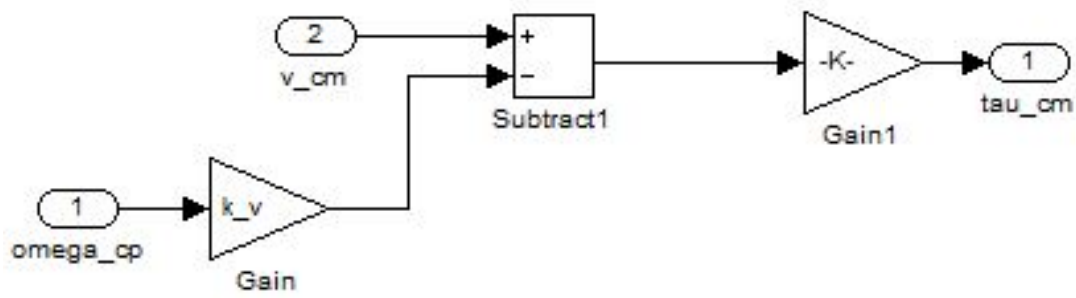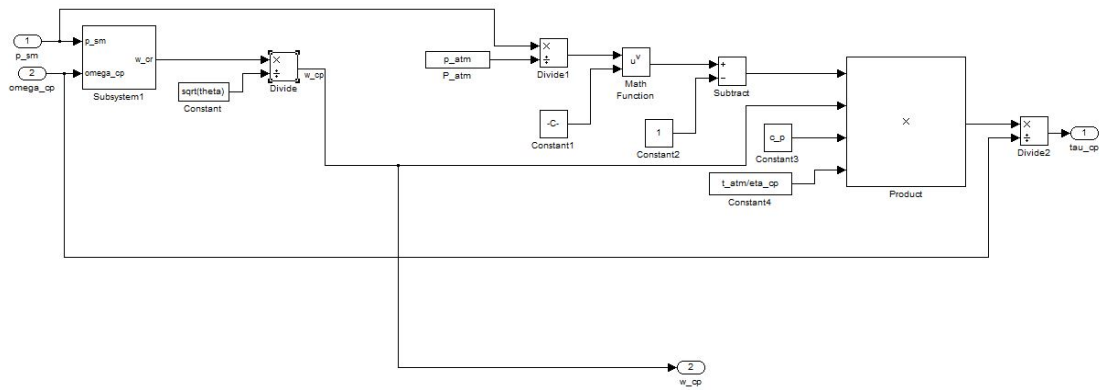### 3.1.1 Compressor

Figure 3.1: Compressor Subsystem

Figure 3.2: Inside the Compressor Subsystem

The masked subsystems generating the compressor motor torque τ_{cm} and torque required to drive the compressor τ_{cp} are presented next.

Figure 3.3: τ_{cm} Subsystem

Figure 3.4: τ_{cp} Subsystem

3.1.2   Supply Manifold

Figure 3.5: Supply Manifold Subsystem

Masked subsystems generating the mass of air in supply manifold m_{sm} and supply manifold pressure p_{sm} are presented below
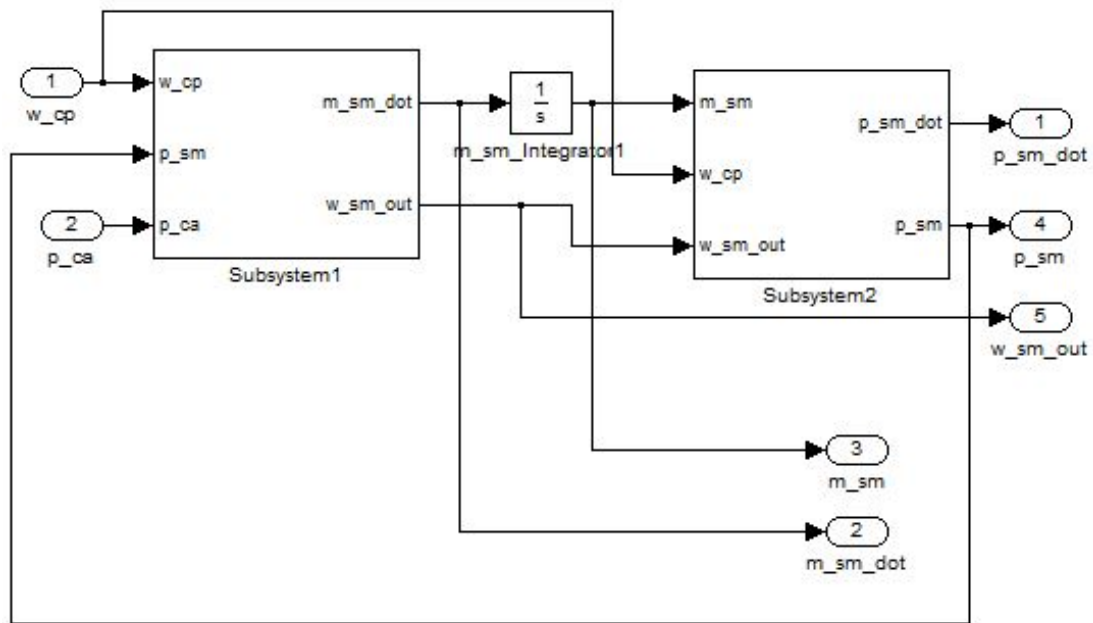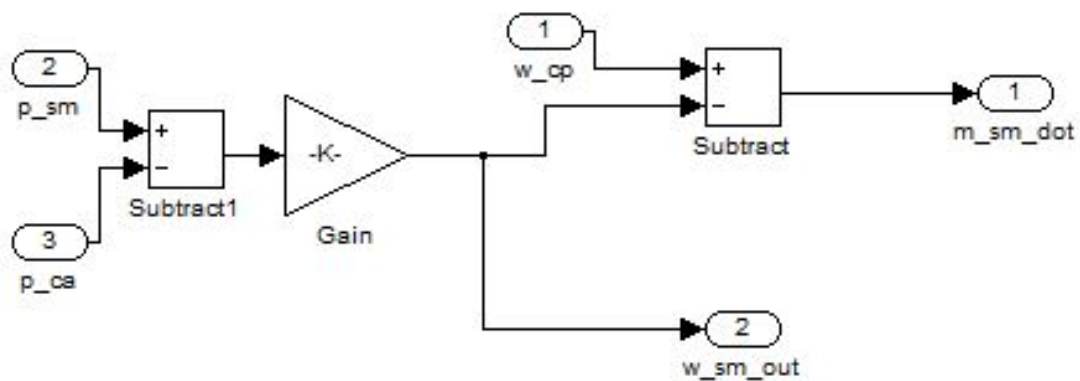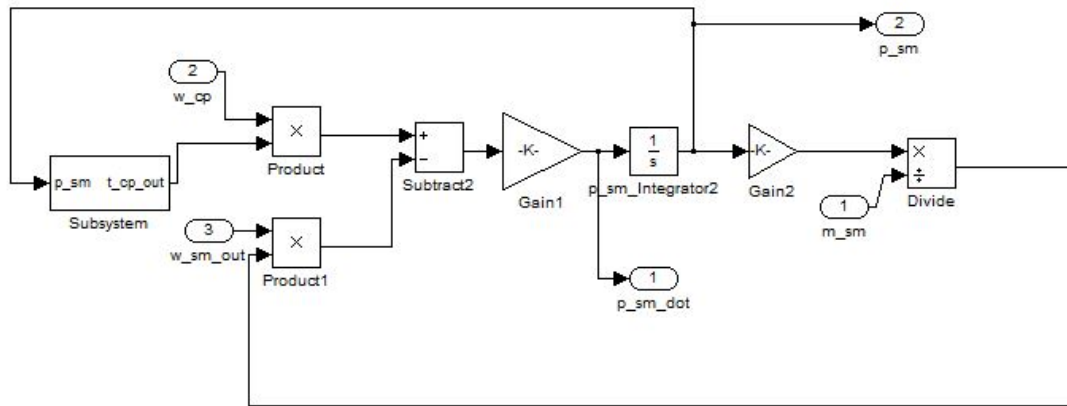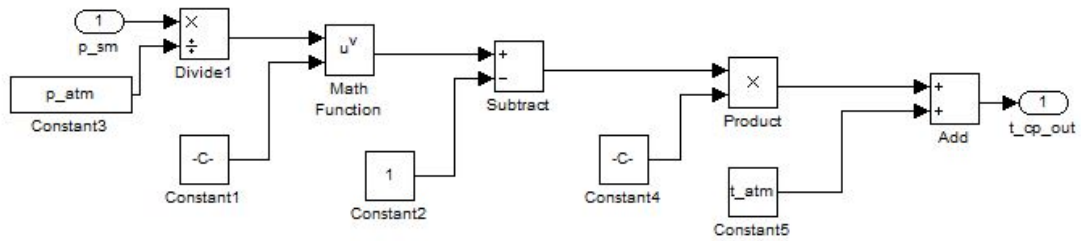
Figure 3.6: Inside the Supply Manifold Subsystem

Figure 3.7: m_{sm} Generating Subsystem

Figure 3.8: P_{sm} Generating Subsystem

The $t_{cp,out}$ is generated as follows

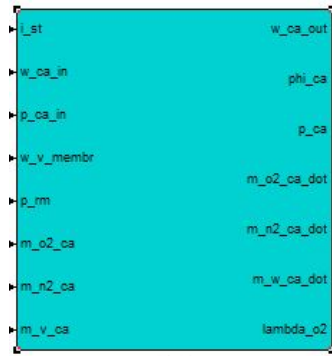Figure 3.9: $t_{cp,out}$ Generating Subsystem

3.1.3 Cathode

Figure 3.10: Cathode Subsystem
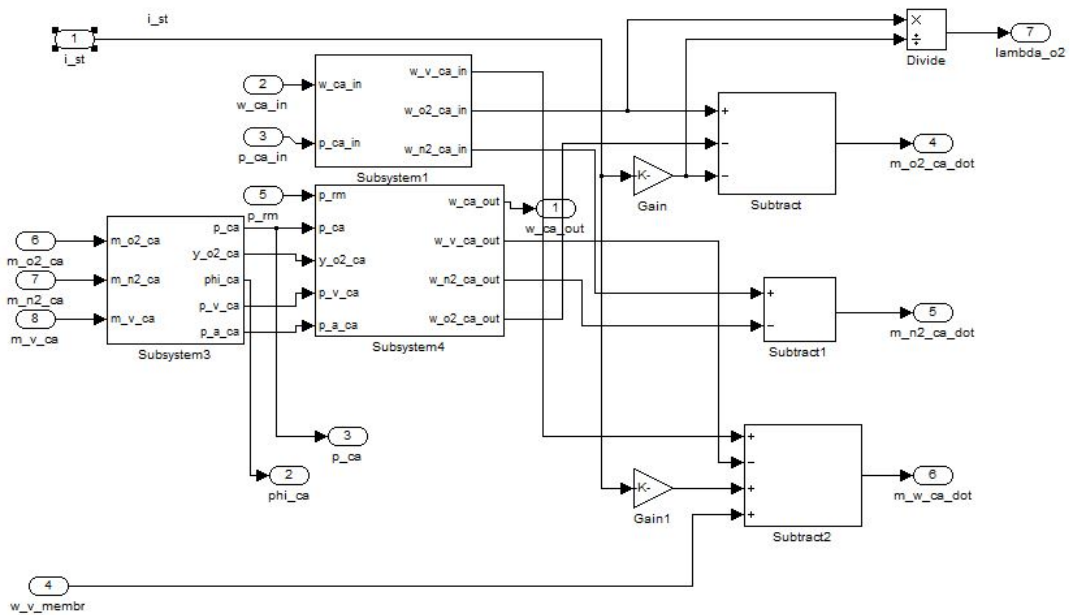
Figure 3.11: Inside the Cathode Subsystem

Here, the SIMULINK block *Subsystem1*,*Subsystem4* and *Subsystem3* generate the inlet flow, outlet flow and other cathode parameters respectively. They have been expanded below:
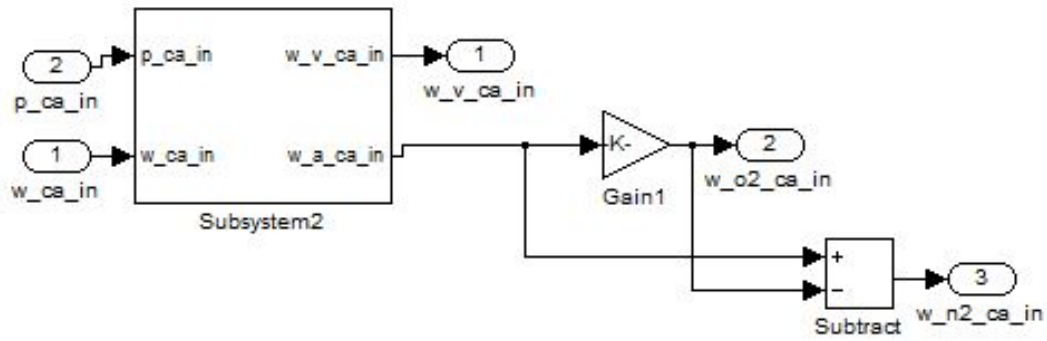
Figure 3.12: O_2 and N_2 Inlet Flow Rate Generating Subsystem
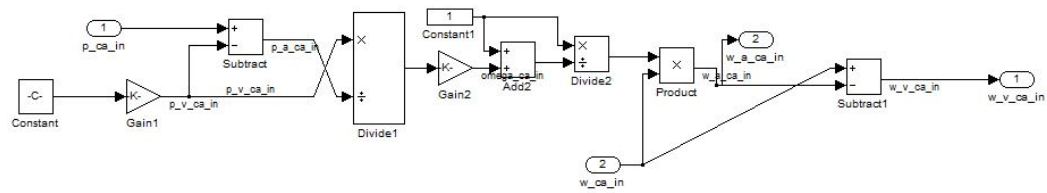
Figure 3.13: Inlet Water Flow Rate Generating Subsystem
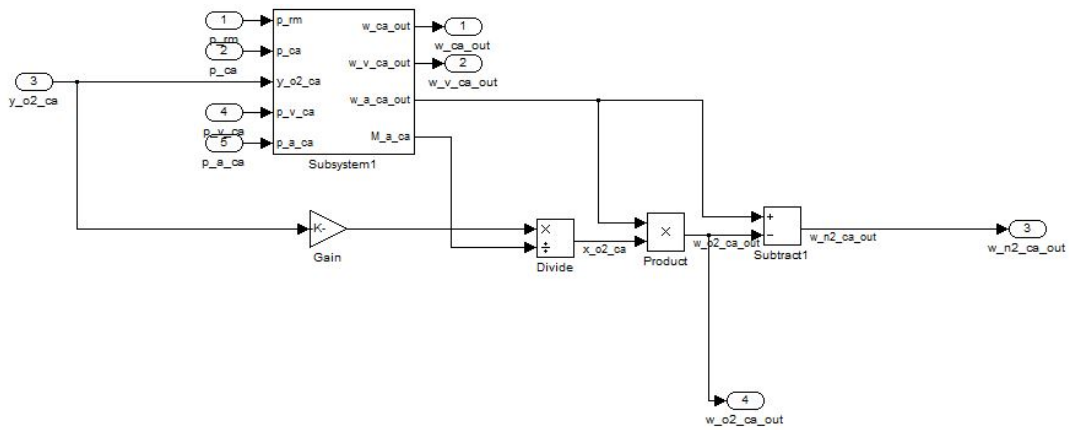
Figure 3.14: O_2 and N_2 Outlet Flow Rate Generating Subsystem
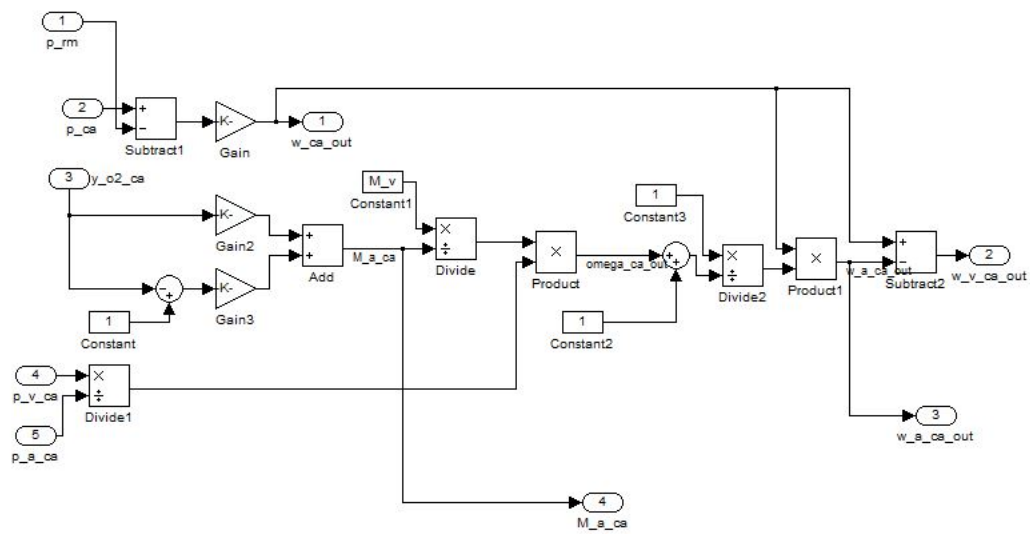
Figure 3.15: Outlet Water Flow Rate Generating Subsystem

3.1.4 Return Manifold
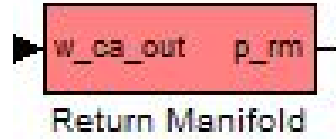
Figure 3.16: Return Manifold Subsystem

The return manifold implementation is simple and straightforward, as presented below:
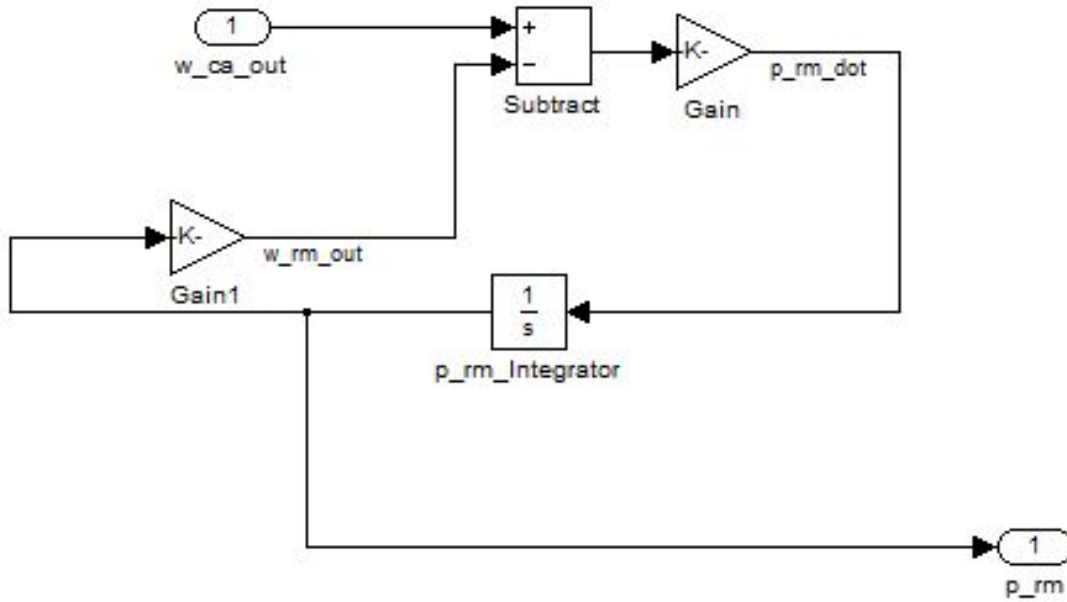
Figure 3.17: Inside the Return Manifold Subsystem

3.1.5 Anode

Similar to cathode, *Subsystem5* and *Subsystem4* are used to compute inlet flow properties and Anode internal properties respectively. Their in-depth implementation is given below:

Figure 3.18: Anode
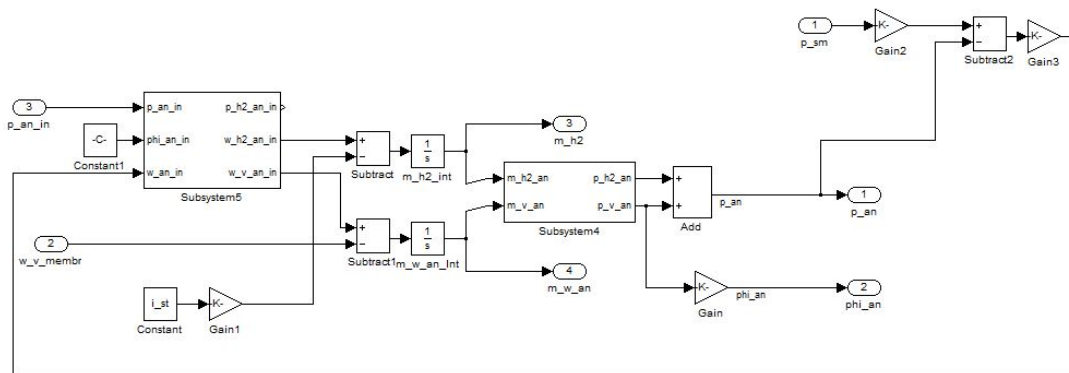
Figure 3.19: Inside the Anode Subsystem
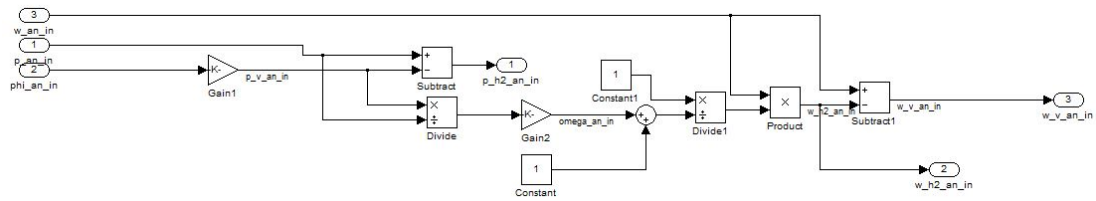
Figure 3.20: Inlet Flow Rate Generating Subsystem
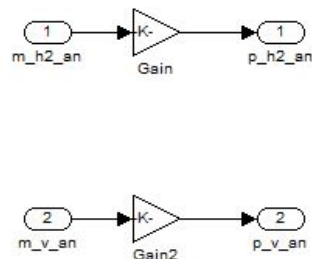
Figure 3.21: Partial Pressure Generating Subsystem

3.1.6   Membrane Hydration
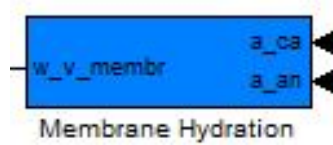
Figure 3.22: Membrane Hydration Model

The membrane hydration is implemented as follows:
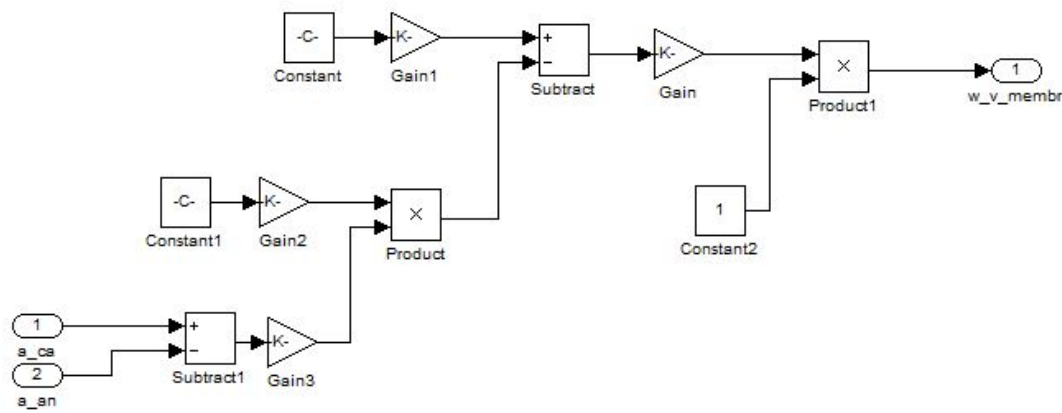
Figure 3.23: Inside the Membrane Hydration Model

3.1.7   PEM Fuel Cell model

All the different SIMULINK blocks presented above can be inter-connected as shown in Figure 3.24 to form the entire PEM fuel cell. Various constants used in the model are presented below

Parameter	Value	Units
R_{O_2}	259.8	–
R_{N_2}	296.8	–
R_v	461.5	–
R_{H_2}	4124.3	–
R_a	286.9	J/(kg.K)
$\bar{R}$	8.3145	J/(mol.K)
M_{O_2}	32×10^{-3}	kg/mol
M_{N_2}	28×10^{-3}	kg/mol
M_v	18.02×10^{-3}	kg/mol
M_{H_2}	2.016×10^{-3}	kg/mol
M_a	28.84×10^{-3}	kg/mol

Table 3.1: Gas Constants and Molar Masses

Parameter	Value	Units
p_{atm}	101325	Pa
T_{atm}	298.15	K
T_{cl}	353	K
T_{st}	353	K
T_{fc}	353	K
ρ_a	1.23	kg/m^3
γ	1.4	–
C_p	1004	J/kg/K
F	96485	Coulombs
ϕ_{des}	1	–
ϕ_{atm}	0.5	–
n	381	–

Table 3.2: Simulation Constants

Figure 3.24: PEM Fuel Cell

3.2 Steady State Operating Point Determination

The PEM fuel cell model in Figure 3.24 was used to determine the system steady state or equilibrium operating point. The overall system has only one input, the compressor motor input voltage, v_{cm}. A steady state value of $164\,\text{V}$ was applied to the system and resulting state values were recorded in MATLAB. Figure 3.25 shows steady state operating points for different states.

Figure 3.25: Steady State Operating Points

These steady state operating points are given by

$Parameter$	$Value$	$Units$
$m_{O_2}^{ss}$	$1.999484727104 \times 10^{-3}$	Kg
$m_{H_2}^{ss}$	$1.106307688879306 \times 10^{-4}$	Kg
$m_{N_2}^{ss}$	$1.3448696345856 \times 10^{-2}$	Kg
ω_{cp}^{ss}	$8.521153438978479 \times 10^{3}$	rad/sec
p_{sm}^{ss}	$2.325384109890503 \times 10^{5}$	Pa
m_{sm}^{ss}	$4.0533533620127 \times 10^{-2}$	Kg
$m_{w,an}^{ss}$	$5.717655072000 \times 10^{-3}$	Kg
$m_{w,ca}^{ss}$	$3.615207662826 \times 10^{-3}$	Kg
p_{rm}^{ss}	$1.927946017884893 \times 10^{5}$	Pa

Table 3.3: Steady State Operating Points

These values are further used in Chapter 4 for Jacobian linearization.

Chapter 4

Control of Linearized Fuel Cell System

4.1 Jacobian Linearization

Jacobian linearization is one of the several techniques used to linearize a non-linear system. It is based on the Taylor series expansion of a non-linear differential equation around a nominal operating point[16].

Consider the following time invariant non-linear dynamical system given by

$$\dot{x}(t) = f(x(t), u(t)) \tag{4.1}$$

$f(t), x(t) \in \mathbf{R^n}, u(t) \in \mathbf{R^m}$

Let $u^o(t)$ be the nominal or steady state input and $x^o(t)$ be the resulting nominal state trajectory. We can approximate the state trajectory around the nominal operating points using the Taylor series expansion as

$$x(t) = x^o(t) + \delta x(t) \tag{4.2}$$

$$u(t) = u^o(t) + \delta u(t) \tag{4.3}$$

$$\dot{x}^o(t) = f(x^o(t), u^o(t)) \tag{4.4}$$

Expanding equation (4.1) using Taylor series we get

$$\dot{x}^o(t) + \delta\dot{x}(t) = f(x^o(t) + \delta x(t), u^o(t) + \delta u(t) \tag{4.5}$$

$$= f(x^o(t), u^o(t)) + \left(\frac{\partial f}{\partial x}\right)\bigg|_{x^o(t), u^o(t)} \delta x(t) + \left(\frac{\partial f}{\partial u}\right)\bigg|_{x^o(t), u^o(t)} \delta u(t) + h.o.t$$

$$\tag{4.6}$$

Where, $h.o.t$ stands for high order terms. Since δx and δu are small, we can neglect the higher order terms.

The matrices of partial derivatives are given by

$$\left(\frac{\partial f}{\partial x}\right)\bigg|_{x^o(t),u^o(t)} = A^{n \times n} = \begin{bmatrix} \frac{\partial f_1}{\partial x_1} & \cdots & \cdots & \frac{\partial f_1}{\partial x_n} \\ \frac{\partial f_2}{\partial x_1} & \cdots & \cdots & \frac{\partial f_2}{\partial x_n} \\ \cdots & \cdots & \cdots & \cdots \\ \frac{\partial f_n}{\partial x_1} & \cdots & \cdots & \frac{\partial f_n}{\partial x_n} \end{bmatrix}\bigg|_{x^o(t),u^o(t)} \quad (4.7)$$

$$\left(\frac{\partial f}{\partial u}\right)\bigg|_{x^o(t),u^o(t)} = B^{n \times m} = \begin{bmatrix} \frac{\partial f_1}{\partial u_1} & \cdots & \cdots & \frac{\partial f_1}{\partial u_m} \\ \frac{\partial f_2}{\partial u_1} & \cdots & \cdots & \frac{\partial f_2}{\partial u_m} \\ \cdots & \cdots & \cdots & \cdots \\ \frac{\partial f_n}{\partial u_1} & \cdots & \cdots & \frac{\partial f_n}{\partial u_m} \end{bmatrix}\bigg|_{x^o(t),u^o(t)} \quad (4.8)$$

The matrices A and B are called Jacobian matrices and are evaluated at nominal/operating points. We can extend the same concept to the output equation as follows.

$$y(t) = g(x(t), u(t)) \quad (4.9)$$

where $y(t), g(t) \in \mathbf{R^p}$.

Applying the Taylor series expansion around $y^o(t)$ in equation (4.9) we have

$$\delta y = \left(\frac{\partial g}{\partial x}\right)\bigg|_{x^o(t),u^o(t)} \delta x(t) + \left(\frac{\partial g}{\partial u}\right)\bigg|_{x^o(t),u^o(t)} \delta u(t) + h.o.t \quad (4.10)$$

Here,

$$\left(\frac{\partial g}{\partial x}\right)\bigg|_{x^o(t),u^o(t)} = C^{p \times n} = \begin{bmatrix} \frac{\partial g_1}{\partial x_1} & \cdots & \cdots & \frac{\partial g_1}{\partial x_n} \\ \frac{\partial g_2}{\partial x_1} & \cdots & \cdots & \frac{\partial g_2}{\partial x_n} \\ \cdots & \cdots & \cdots & \cdots \\ \frac{\partial g_p}{\partial x_1} & \cdots & \cdots & \frac{\partial g_p}{\partial x_n} \end{bmatrix}\bigg|_{x^o(t),u^o(t)} \quad (4.11)$$

$$\left(\frac{\partial g}{\partial u}\right)\bigg|_{x^o(t),u^o(t)} = D^{p \times m} = \begin{bmatrix} \frac{\partial g_1}{\partial u_1} & \cdots & \cdots & \frac{\partial g_1}{\partial u_m} \\ \frac{\partial g_2}{\partial u_1} & \cdots & \cdots & \frac{\partial g_2}{\partial u_m} \\ \cdots & \cdots & \cdots & \cdots \\ \frac{\partial g_p}{\partial u_1} & \cdots & \cdots & \frac{\partial g_p}{\partial u_m} \end{bmatrix}\bigg|_{x^o(t),u^o(t)} \quad (4.12)$$

Combining the results from equation (4.7),(4.8),(4.11),(4.12) we can write

$$\delta \dot{x}(t) = A\delta x(t) + B\delta u(t) \tag{4.13}$$

$$\delta y(t) = C\delta x(t) + D\delta u(t) \tag{4.14}$$

The above equations are linearized versions of the non-linear equations (4.1) and (4.9)

4.2   Linearized Model

MATLAB symbolic toolbox is used for Jacobian linearization. All the non-linear equations from (2.80) to (2.88) are expressed as symbolic equations in MATLAB and the command `jacobian()` does the linearization. The linearized symbolic model is then evaluated at the steady state operating point presented in Table 3.3. MATLAB code for achieving the linearization is presented below.

```
% Define the symbolic variables
syms x1 x2 x3 x4 x5 x6 x7 x8 x9 u i_st


% Write the non-linear equations in terms of symbolic variables
%state equations
f1=((y_o2_ca_in*M_o2/(y_o2_ca_in*M_o2+(1-y_o2_ca_in)*M_n2))*...


f2=((1/(1+((M_v/M_h2)*((phi_an_in*((10^(-1.69*10^-10*t_an_in^4+...
.
.
.
f9=(R_a*T_rm/v_rm)*((k_ca_out*(((x1*R_o2+x3*R_n2+x8*R_v)*t_st/v_ca)-x9))-...


%output equations
g1=(((((a_4*(((pi/60)*d_c*(((60*x4)/(2*pi))/sqrt(theta)))/sqrt(1.4*298*2.869*100))^4+...
g2=x5
g3=n*((1.229-8.5*10^-4*(t_fc-298.15)+4.308*10^-5*t_fc*...
```

```
% Linearize the equations

A=jacobian([f1; f2; f3; f4; f5; f6; f7; f8; f9],[x1 x2 x3 x4 x5 x6 x7 x8 x9]);

B=jacobian([f1; f2; f3; f4; f5; f6; f7; f8; f9],u);

C=jacobian([g1; g2; g3],[x1 x2 x3 x4 x5 x6 x7 x8 x9]);

D=jacobian([g1; g2; g3],u);


% Define the steady state values

x1=0.001999484727104;

x2=1.106307688879306e-004;

x3=0.013448696345856;

x4=8.521153438978479e+003;

x5=2.325384109890503e+005;

x6=0.040533533620127;

x7=0.005717655072000;

x8=0.003615207662826;

x9=1.927946017884893e+005;


%Evaluate the matrices

A=eval(A);

B=eval(B);

C=eval(C);

D=eval(D);
```

The linearization results are as follows:

$$
A = \begin{bmatrix}
-13.1969 & 0 & -11.8130 & 0 & 92.2081 & 0 & 0 & -18.5365 & 22.8385 \\
0 & -6.1101\times10^5 & 0 & 0 & 1.9725\times10^5 & 0 & -6.8370\times10^4 & 0 & 0 \\
-40.0581 & 0 & -48.9479 & 0 & 303.5182 & 0 & 0 & -72.7422 & 153.5547 \\
0 & 0 & 0 & -16.0045 & 184.5824 & 0 & 0 & 0 & 0 \\
2.6731 & 0 & 3.0538 & 0.5052 & -40.8247 & 0.1036 & 0 & 4.7483 & 0 \\
33.2813 & 0 & 38.0212 & 6.3240 & -449.1373 & 0 & 0 & 59.1199 & 0 \\
0 & -463.1732 & 0 & 0 & 149.5259 & 0 & -51.8281 & 1.1402 & 0 \\
-3.5133 & 0 & -4.0921 & 0 & 3.0008 & 0 & 0 & -10.7027 & 41.3067 \\
4.0440 & 0 & 4.6199 & 0 & 0 & 0 & 0 & 7.1836 & -50.4044
\end{bmatrix}
$$

$$(4.15)$$

$$
B = \begin{bmatrix}
0 \\
0 \\
0 \\
3.4922 \\
0 \\
0 \\
0 \\
0 \\
0
\end{bmatrix}
$$

$$
C = \begin{bmatrix}
0 & 0 & 0 & 0.0063 & -131.2373 & 0 & 0 & 0 & 0 \\
0 & 0 & 0 & 0 & 1 & 0 & 0 & 0 & 0 \\
19.7004 & 52.3720 & -0.5182 & 0 & 0 & 0 & 0 & -0.8057 & 0
\end{bmatrix}
$$

$$
D = \begin{bmatrix} 0 \\ 0 \\ 0 \end{bmatrix}
$$

Note that the linearized fuel cell model is a 9th order model. The next chapter discusses Controllability, Observability and Stability issues of this model.

Chapter 5

System Analysis

This chapter discusses stability, controllability, and observability of the linearized PEM fuel cell model presented in Chapter 4.

5.1 Stability Analysis of Linearized PEM Fuel Cell Model

The eigenvalues of the system matrix A are

$$\lambda(A) = \begin{bmatrix} -6.1105 \times 10^5 \\ -104.64 \\ -46.7355 \\ -17.5058 \\ -4.1091 \\ -2.8769 + 0.0726i \\ -2.8769 - 0.0726i \\ -1.3322 \\ -1.0481 \times 10^{-15} \end{bmatrix} \tag{5.1}$$

Though one of the eigenvalue is very small and is very close to the origin, the system is still asymptotically stable. Next section examines controllability and observability of the fuel cell system.

5.2 Controllability and Observability test

For the eigenvalue placement feedback control technique, the system has to be controllable. For designing observers the system has to be observable. There are several tests to determine whether the given linear dynamical system is controllable (observable) or

not, like the grammiam test, rank of controllability (observability) matrix etc. [16]. But the most elegant tests are the Popov Belevitch eigenvalue and eigenvector tests. These tests are very accurate over other tests and are highly recommended in environments like MATLAB, where the possibility of numerical precision errors are not in the programmer's control.

5.2.1   Popov Belevitch Eigenvalue Test

This theorem states that a system is controllable if the matrix

$$[A - \lambda I \ B]$$

has full rank for every λ where $\lambda = \text{eig}(A)$, i.e.

$$\text{rank}[A - \lambda_i I \ B] = n \quad \forall \lambda_i(A), i = 1, 2..., n$$

The test, as applied to the fuel cell model (4.15), is presented below.

Controllability of Linearized PEM Fuel Cell

$$\text{rank}[A - \lambda_1 I \ B] = 9 \tag{5.2}$$

$$\text{rank}[A - \lambda_2 I \ B] = 9 \tag{5.3}$$

$$\text{rank}[A - \lambda_3 I \ B] = 9 \tag{5.4}$$

$$\text{rank}[A - \lambda_4 I \ B] = 9 \tag{5.5}$$

$$\text{rank}[A - \lambda_5 I \ B] = 9 \tag{5.6}$$

$$\text{rank}[A - \lambda_6 I \ B] = 9 \tag{5.7}$$

$$\text{rank}[A - \lambda_7 I \ B] = 9 \tag{5.8}$$

$$\text{rank}[A - \lambda_8 I \ B] = 9 \tag{5.9}$$

$$\text{rank}[A - \lambda_9 I \ B] = 9 \tag{5.10}$$

From (5.2)-(5.10), it is clear that the linearized model (4.15) is completely controllable.

Observability of Linearized PEM Fuel Cell

Popov Belevitch test for observability states that: A system is observable if,

$$\text{rank} \begin{bmatrix} \lambda_i I - A \\ C \end{bmatrix} = n \quad \forall \lambda_i(A), i = 1, 2..., n$$

This test, as applied to the linearized fuel cell model, is presented below.

$$\text{rank} \begin{bmatrix} \lambda_1 I - A \\ C \end{bmatrix} = 9 \tag{5.11}$$

$$\text{rank} \begin{bmatrix} \lambda_2 I - A \\ C \end{bmatrix} = 9 \tag{5.12}$$

$$\text{rank} \begin{bmatrix} \lambda_3 I - A \\ C \end{bmatrix} = 9 \tag{5.13}$$

$$\text{rank} \begin{bmatrix} \lambda_4 I - A \\ C \end{bmatrix} = 9 \tag{5.14}$$

$$\text{rank} \begin{bmatrix} \lambda_5 I - A \\ C \end{bmatrix} = 9 \tag{5.15}$$

$$\text{rank} \begin{bmatrix} \lambda_6 I - A \\ C \end{bmatrix} = 9 \tag{5.16}$$

$$\text{rank} \begin{bmatrix} \lambda_7 I - A \\ C \end{bmatrix} = 9 \tag{5.17}$$

$$\text{rank} \begin{bmatrix} \lambda_8 I - A \\ C \end{bmatrix} = 9 \tag{5.18}$$

$$\text{rank} \begin{bmatrix} \lambda_9 I - A \\ C \end{bmatrix} = 9 \tag{5.19}$$

Obviously, from (5.11)-(5.19), (4.15) is completely observable.

5.2.2 Popov Belevitch Eigenvector Test

This is another elegant test for determining whether a system is controllable (observable) or not. The controllability test says that, a system is controllable if, no left

eigenvector of A is orthogonal to B [17].

i.e. if v^* is the left eigenvector of A, corresponding to any λ then

$$v^*A = v^*\lambda$$

$$\Rightarrow v^*B \neq 0$$

Controllability of Linearized PEM Fuel Cell

The controllability of the linearized 9th order PEM fuel cell model in (4.15) is determined using the Popov Belevitch eigenvector test. The resulting vectors v^*B for controllability

$$v_1^*B = 8.8212e - 007 \neq 0 \tag{5.20}$$

$$v_2^*B = -0.0154 \neq 0 \tag{5.21}$$

$$v_3^*B = -0.0460 \neq 0 \tag{5.22}$$

$$v_4^*B = 0.5730 \neq 0 \tag{5.23}$$

$$v_5^*B = 0.0792 \neq 0 \tag{5.24}$$

$$v_6^*B = 0.0728 - 0.0019i \implies ||v_6^*B|| = 0.0728 \neq 0 \tag{5.25}$$

$$v_7^*B = 0.0728 + 0.0019i \implies ||v_7^*B|| = 0.0728 \neq 0 \tag{5.26}$$

$$v_8^*B = 0.0032 \neq 0 \tag{5.27}$$

$$v_9^*B = 0.0017 \neq 0 \tag{5.28}$$

Where, v_i^* is the left eigenvector corresponding to λ_i. The above results confirms the conclusion obtained in the previous section.

Note: The Popov Belevitch eigenvector test can not give the controllability measure of a particular state variable.

Observability of Linearized PEM Fuel Cell

The results presented above can be extended to observability. For a system to be observable [17],

$$Cx_i \neq 0 \quad \text{for } Ax_i = \lambda x_i \quad i = 1, 2, ..., n$$

Cx_i for the observability test are presented below.

$$Cx_1 = [0 \quad 0 \quad 52.3720]^T \implies ||Cx_1|| = 52.3720 \neq 0 \tag{5.29}$$

$$Cx_2 = [-6.4719 \quad 0.0493 \quad -2.3561]^T \implies ||Cx_2|| = 6.8876 \neq 0 \tag{5.30}$$

$$Cx_3 = [9.1423 \quad -0.0696 \quad 0.9599]^T \implies ||Cx_3|| = 9.1928 \neq 0 \tag{5.31}$$

$$Cx_4 = [1.0427 \quad -0.0079 \quad -1.5757]^T \implies ||Cx_4|| = 1.8895 \neq 0 \tag{5.32}$$

$$Cx_5 = [-5.0079 \quad 0.0382 \quad -1.1778]^T \implies ||Cx_5|| = 5.1447 \neq 0 \tag{5.33}$$

$$Cx_6 = [-5.160 - 0.028i \quad 0.039 + 0.0002i \quad -2.055 + 7.096i]^T \tag{5.34}$$

$$\implies ||Cx_6|| = 9.0116 \neq 0 \tag{5.35}$$

$$Cx_7 = [-5.1603 + 0.0285i \quad 0.0393 - 0.0002i \quad -2.0555 - 7.0959i]^T \tag{5.36}$$

$$\implies ||Cx_7|| = 9.0116 \neq 0 \tag{5.37}$$

$$Cx_8 = [2.6632 \quad -0.0203 \quad -1.0124]^T \implies ||Cx_8|| = 2.8492 \neq 0 \tag{5.38}$$

$$Cx_9 = [0 \quad 0 \quad 5.8240]^T \implies ||Cx_9|| = 5.8240 \neq 0 \tag{5.39}$$

Where, x_i is the eigenvector corresponding to λ_i

It can be seen from (5.29)-(5.39) that the fuel cell model is completely observable.

Note: The Popov Belevitch eigenvector test can not give the observability measure of a particular state variable.

5.3 Model Reduction

If the state of a system is weakly controllable and weakly observable, it can be discarded from the model without affecting the system dynamics to a reasonable extent. This technique is called system order reduction [16].

One of the methods to achieve model reduction is through balanced transformation or simply balancing. Balancing is a similarity transformation that puts the system such that its controllability and observability grammiams are identical and diagonal, with Hankel singular values on the diagonal of the grammiam matrix [18]. Hankel singular values give the controllability and observability measure of each state. The Hankel

singular values of the fuel cell model presented in (4.15) is presented below

$$\sigma = \begin{bmatrix} \infty & & & & & & & & \\ & 1.281038 & & & & & & & \\ & & 0.098375 & & & & & & \\ & & & 0.032746 & & & & & \\ & & & & 0.009357 & & & & \\ & & & & & 0.002487 & & & \\ & & & & & & 0.000160 & & \\ & & & & & & & 0.000121 & \\ & & & & & & & & 3.9915\times10^{-11} \end{bmatrix} \tag{5.40}$$

The last singular value being extremely small, indicates the presence of a weakly controllable and weakly observable mode, and can be removed from the system dynamics.

5.3.1 Truncated Model

The original 9th order model has been reduced to an 8th order model using balanced truncation. The model is presented below:

$$A_r = \begin{bmatrix} 8.755\times10^{-16} & 0 & 0 & 0 & 0 & 0 & 0 & 0 \\ 0 & -2.022 & -4.074 & -0.4982 & 1.01 & 0.1089 & -0.1858 & -0.03214 \\ 0 & 4.11 & -23.21 & -4.301 & 7.687 & 1.374 & -1.79 & -0.3882 \\ 0 & 0.7252 & -7.28 & -2.456 & -6.442 & 0.7262 & 0.4688 & -0.1478 \\ 0 & -1.729 & 20.32 & 13.71 & -50.17 & 0.9117 & 18.26 & 1.065 \\ 0 & -0.1221 & 1.456 & 0.785 & -7.346 & -0.9462 & 0.428 & 0.4205 \\ 0 & 0.3187 & -3.894 & -2.199 & 18.26 & 4.92 & -99.93 & 7.984 \\ 0 & 0.03214 & -0.3924 & -0.2209 & 1.859 & 0.4783 & -26.18 & -1.345 \end{bmatrix} \tag{5.41}$$

$$B_r = \begin{bmatrix} 0.05898 \\ 2.276 \\ -2.137 \\ -0.401 \\ 0.9689 \\ 0.0686 \\ -0.1794 \\ -0.01809 \end{bmatrix}$$

$$C_r = \begin{bmatrix} 8.357\times10^{-14} & -2.089 & -1.821 & -0.1303 & 0.8284 & 0.04379 & -0.1538 & -0.01662 \end{bmatrix}$$

$$D_r = 0 \tag{5.42}$$

The eigen values of the truncated system are:

$$\lambda(A_r) = \begin{bmatrix} -104.6445 \\ -46.7355 \\ -17.5058 \\ -1.3322 \\ -4.1091 \\ -2.8769 + 0.0726i \\ -2.8769 - 0.0726i \\ 8.7553 \times 10^{-16} \end{bmatrix} \tag{5.43}$$

This system is controllable and observable with respect to all the eigenvalues. The claim has been verified using Popov Belevitch test.

Comments: State x_9 is truncated from the balanced system. The next step is to determine the relation between the eliminated x_9 in the balanced coordinate and the states in the original coordinate system. The similarity transformation matrix T in the transformation, $x_b = Tx$ is used to determine the relation. The subscript b indicates the balanced system.

$$x_{9,b} = -0.0103x_1 - 7496.7023x_2 - 0.0120x_3 - 0.0019x_4 + 2420.3164x_5$$
$$- 0.00042x_6 - 838.8643x_7 - 0.0170x_8 - 0.00051x_9 \tag{5.44}$$

From equation (5.44), one things that stands out is $x_{9,b}$ is predominantly dependent on mass of hydrogen in anode, x_2; pressure of gas in supply manifold, x_5, and mass of water in anode, x_7.

$$x_{9,b} \approx -7496.7023x_2 + 2420.3164x_5 - 838.8643x_7 \tag{5.45}$$

It seems like one of these three states is weakly controllable and weakly observable. To get a better picture of the scenario, the system needs to be analysed in a new coordinate system, which is presented in the next section.

5.4 Modal Transformation

The intention of this section is to get a more clear picture, if possible, to determine which state in original state space coordinates is weakly controllable and weakly observable

based on the observations from the truncated system in (5.41). The modal transformation is a similarity transformation that generates a diagonal system matrix A. It gives a nice decoupled system equation. The transformation matrix P in $z = P^{-1}x$ that does this is simply the eigenvector matrix of A. The system (4.15) in modal coordinates is presented below:

$$\bar{A} = \begin{bmatrix} -6.1105 \times 10^5 \\ & -104.64 \\ & & -46.7355 \\ & & & -17.5058 \\ & & & & -4.1091 \\ & & & & & -2.8769 + 0.0726i \\ & & & & & & -2.8769 - 0.0726i \\ & & & & & & & -1.3322 \\ & & & & & & & & -1.0481 \times 10^{-15} \end{bmatrix}$$

$$(5.46)$$

$$\bar{B} = \begin{bmatrix} 9.32117816810097 \times 10^{-7} \\ -0.0698 \\ 0.3544 \\ 2.734 \\ -0.2987 \\ 0.7899 - 0.4771i \\ 0.7899 + 0.4771i \\ 0.0606 \\ -0.0018 \end{bmatrix}$$

$$\bar{C} = \begin{bmatrix} 3.6285 \times 10^{-17} & -6.4719 & 9.1423 & 1.0427 & -5.0078 & -5.1603 - 0.0285i & -5.1603 + 0.0285i & 2.6632 & 3.6324 \times 10^{-13} \\ 0 & 0.0493 & -0.0696 & -0.0078 & 0.03818 & 0.0393 + 0.00021i & 0.0393 - 0.00021i & -0.0203 & -2.7694 \times 10^{-15} \\ 52.372 & -2.3560 & 0.9598 & -1.5757 & -1.1778 & -2.0554 + 7.0958i & -2.0554 - 7.0958i & -1.0123 & 5.8239 \end{bmatrix}$$

From the modal transformation, we get nine decoupled system equations given by

$$\dot{z}_i = \lambda_i z_i + \beta_i u_i \qquad (5.47)$$

$$y_i = \gamma_i z_i \qquad \forall i = 1, 2...9$$

The Hankel singular values of all nine decoupled systems are:

$$\sigma_{z_1} = 3.9945 \times 10^{-11} \tag{5.48}$$

$$\sigma_{z_2} = 0.0023 \tag{5.49}$$

$$\sigma_{z_3} = 0.0349 \tag{5.50}$$

$$\sigma_{z_4} = 0.1476 \tag{5.51}$$

$$\sigma_{z_5} = 0.1870 \tag{5.52}$$

$$\sigma_{z_6} = 1.4453 \tag{5.53}$$

$$\sigma_{z_7} = 1.4453 \tag{5.54}$$

$$\sigma_{z_8} = 0.0649 \tag{5.55}$$

$$\sigma_{z_9} = \infty \tag{5.56}$$

Observe that the order of magnitude of the singular values in the modal coordinate are almost similar to that of the balanced system.

Comments: Out of the nine system equations, the state variable z_1 corresponds to smallest Hankel Singular Value after balancing, with the corresponding singular value $\sigma = 3.9945 \times 10^{-11}$. The transformation relating z_1 and the original state space coordinates is

$$\begin{aligned} z_1 = &\, 1.412 \times 10^{-6} x_1 + 0.999 x_2 + 1.613 \times 10^{-6} x_3 + 2.669 \times 10^{-7} x_4 - 0.322 x_5 \\ &+ 5.471 \times 10^{-8} x_6 + 0.112 x_7 + 2.3 \times 10^{-6} x_8 - 6.138 \times 10^{-10} x_9 \end{aligned} \tag{5.57}$$

Again, z_1 predominantly depends on a linear combination of x_2, x_5, x_7, which is consistent with the conclusion obtained in the previous section.

$$z_1 \approx 0.999 x_2 - 0.322 x_5 + 0.112 x_7 \tag{5.58}$$

Conclusion: Equations (5.45) and (5.58) suggest that either one or more of x_2, x_5 or x_7 is both weakly controllable and observable. Since the weight of x_2 is more, it seems reasonable to say that x_2 is weakly controllable and weakly observable. But, this statement is counter-intuitive, because x_2 is mass of hydrogen gas in anode, which is the key part of fuel cell dynamics. Since the state space model is not unique and it does not preserve the units of the states, it is very difficult in general to determine

which state in the original coordinate is weakly controllable and weakly observable by looking at the balanced or modal coordinates.

Chapter 6

Controller Design

This chapter discusses simple pole placement control design for the linearized PEM fuel cell model (4.15). Stack current acts as a disturbance in the fuel cell model, but is not considered in this work.

6.1 Eigenvalue Assignment Controller

If the system is controllable, its eigen values can be assigned at any desired location in the s-plane using state feedback [16]. If all the states are not available directly for feedback, an observer can be designed to estimate the states and these estimates can, in turn, be used for state feedback, provided the system is observable.

Consider a linear dynamical system in state space form as

$$\dot{x}(t) = Ax(t) + Bu(t) \tag{6.1}$$

$$y(t) = Cx(t) + Du(t) \tag{6.2}$$

Assuming all states are readily available for feedback, we can write $u(t) = -Kx(t)$, where K is feedback gain vector. The value of K depends on the desired values of the closed-loop eigenvalues.

With state feedback, we can write (6.2) as

$$\dot{x}(t) = (A - BK)x(t)$$

$$\implies x(t) = e^{(A-BK)t}x_0, \quad x_0 \text{ is the initial condition of the states} \tag{6.3}$$

Equation (6.3) implies that the eigenvalues of the matrix $A - BK$ decide the transient response of the system. Hence, to achieve faster convergence to steady state, the eigenvalues of $A - BK$ should be placed to the left half of the s-plane. The farther the

eigenvalue from the origin on negative half of s-plane, the faster will be the transient response, i.e. $Re\{\lambda(A - BK) \ll 0\}$.

In many practical applications, the intention is to lead the states to their respective steady state values quickly. The equation $u(t) = -Kx(t)$, leads all the states to zero. Hence, for practical purposes the equation of state feedback is modified as $u(t) = u_0 - Kx(t)$, where u_0 is the input corresponding to the desired steady state values of the system. Following figure depicts the full state feedback as implemented in SIMULINK.
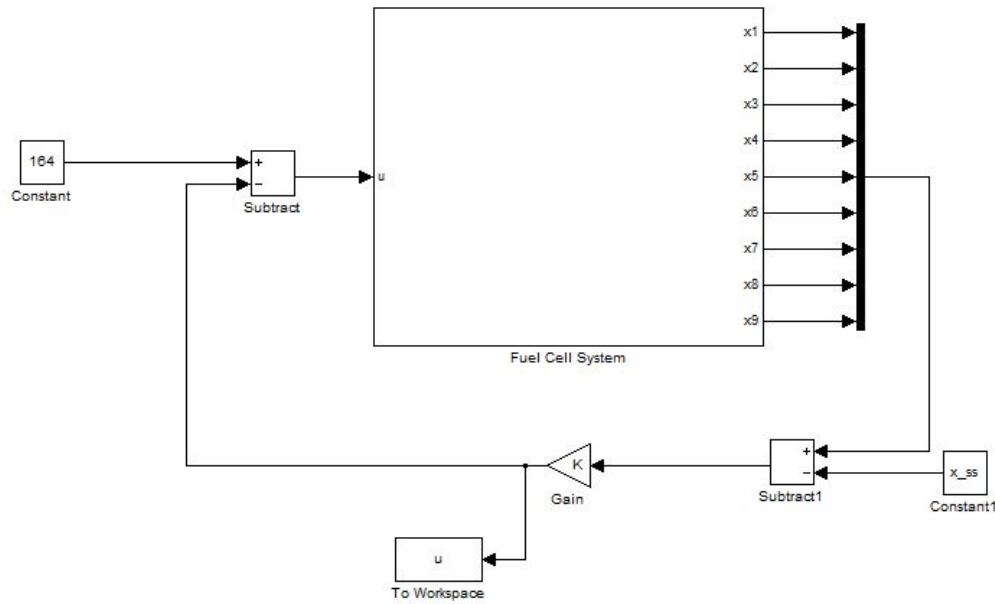

Figure 6.1: Pole Placement Control Design

The pole placement controller is designed for the linear plant and is applied to the non-linear plant. The eigenvalues used for eigenvalue assignment and the resulting gain matrix K is given below:

$$\lambda^{desired} = \begin{bmatrix} -6.1106 \times 10^5, -200, -100, -50, -25, -20, -3, -2, -1 \end{bmatrix} \tag{6.4}$$

$$K = \begin{bmatrix} -820.345, & -317.860, & -270.734, & 63.259, & 69878.457, & -5224.392, & 419312.572, & 122743.826, & 99979.740 \end{bmatrix} \tag{6.5}$$

This controller is designed assuming all states are available for feedback, which is not actually the case. In fact, it's evident from the output equation in (4.15) that

only x_5 is directly available from the measurement. Rest of the eight states need to be extracted from the measurement, using observers.

Chapter 7

Conclusions and Future Work

7.1 Conclusions

This thesis goes about developing a 9th order linear model of PEM fuel cells. The Pukrushpans non-linear model [3] is used for linearization. Simulations are carried out to determine the steady state operating values of the model and are subsequently used in Jacobian linearization. The linearized model is controllable and observable with respect to all the states and requires no order reduction. This model represents the system dynamics in a more comprehensive and accurate manner. A pole-placement controller is incorporated to achieve desired transient response from the system.

7.2 Future Work

In this thesis, we have assumed that all the states are directly measurable. In reality though, the output equations suggest that only the state $x_5 = P_{sm}$ is available for direct measurement. Hence, for pole placement we need a state observer that will estimate the other 8 states. Since, the system is completely observable, we can design an observer and can use the estimated states needed for pole placement. Further, stack current acts as a disturbance for the fuel cell system. We can add an integral control in addition to pole placement controller to remove the effects of disturbance.

In non-linear realm, a sliding mode control strategy can also be applied to the system, without even linearizing it. Evidently, this work has been carried out on 5th order non-linear model [15]. Works by [12][14][13] also deal with sliding mode control of PEM fuel cells.

References

[1] Frano Barbir. *PEM Fuel Cells: Theory and Practice.* Academic Press, 2012.

[2] L Carrette, K A Friedrich, and U Stimming. Fuel cells–fundamentals and applications. *Fuel Cells*, 1(1):5–39, 2001.

[3] J T Pukrushpan, A G Stefanopoulou, and H Peng. *Control of Fuel Cell Power Systems: Principles, Modeling, Analysis and Feedback Design.* Springer Science & Business Media, 2004.

[4] J Padulles, G W Ault, and J R McDonald. An integrated SOFC plant dynamic model for power systems simulation. *Journal of Power sources*, 86(1):495–500, 2000.

[5] M Y El-Sharkh, A Rahman, M S Alam, P C Byrne, A A Sakla, and T Thomas. A dynamic model for a stand-alone PEM fuel cell power plant for residential applications. *Journal of Power Sources*, 138(1):199–204, 2004.

[6] R Gemmen. Analysis for the effect of inverter ripple current on fuel cell operating condition. *Journal of Fluids Engineering*, 125(3):576–585, 2003.

[7] L Y Chiu, B Diong, and R S Gemmen. An improved small-signal model of the dynamic behavior of PEM fuel cells. *Industry Applications, IEEE Transactions on*, 40(4):970–977, 2004.

[8] W K Na and B Gou. Feedback-linearization-based nonlinear control for PEM fuel cells. *Energy Conversion, IEEE Transactions on*, 23(1):179–190, 2008.

[9] M Grujicic, K M Chittajallu, E H Law, and J T Pukrushpan. Model-based control strategies in the dynamic interaction of air supply and fuel cell. *Proceedings of*

the Institution of Mechanical Engineers, Part A: Journal of Power and Energy, 218(7):487–499, 2004.

[10] M Grujicic, K M Chittajallu, and J T Pukrushpan. Control of the transient behaviour of polymer electrolyte membrane fuel cell systems. *Proceedings of the Institution of Mechanical Engineers, Part D: Journal of Automobile Engineering*, 218(11):1239–1250, 2004.

[11] J T Pukrushpan, H Peng, and A G Stefanopoulou. Control-oriented modeling and analysis for automotive fuel cell systems. *Journal of Dynamic Systems, Measurement, and Control*, 126(1):14–25, 2004.

[12] P C Chen. Robust voltage tracking control for proton exchange membrane fuel cells. *Energy Conversion and Management*, 65:408–419, 2013.

[13] A Pilloni, A Pisano, and E Usai. Observer based air excess ratio control of a PEM fuel cell system via high order sliding mode. August 2015.

[14] C Kunusch, P Puleston, M Mayosky, J Riera, et al. Sliding mode strategy for PEM fuel cells stacks breathing control using a super-twisting algorithm. *Control Systems Technology, IEEE Transactions on*, 17(1):167–174, 2009.

[15] G Park and Z Gajic. A simple sliding mode controller of a fifth-order nonlinear PEM fuel cell model. *Energy Conversion, IEEE Transactions on*, 29(1):65–71, 2014.

[16] C Chen. *Linear System Theory and Design*. Oxford University Press, Inc., 1999.

[17] Kemin Zhou and John Comstock Doyle. *Essentials of robust control*, volume 180. Prentice hall Upper Saddle River, NJ, 1998.

[18] Z Gajic and M Lelic. Improvement of system order reduction via balancing using the method of singular perturbations. *Automatica*, 37(11):1859–1865, 2001.

[19] G Park and Z Gajic. Sliding mode control of a linearized polymer electrolyte membrane fuel cell model. *Journal of Power Sources*, 212:226–232, 2012.

[20] C Kunusch, P Puleston, and M Mayosky. *Sliding-Mode Control of PEM Fuel Cells.* Springer Science & Business Media, 2012.

[21] D Feroldi and M Basualdo. Description of PEM fuel cells system. In *PEM Fuel Cells with Bio-Ethanol Processor Systems.* pp. 49-72. Springer, 2012.

[22] M Nabag and M Bettayeb. Overview of nonlinear dynamic modeling of PEM fuel cell systems for control purposes. *International Conference on Renewable Energy: Generation and Applications, ALAM, UAE*, March 2012.

[23] J T Pukrushpan, A G Stefanopoulou, S Varigonda, J Eborn, and C Haugstetter. Control-oriented model of fuel processor for hydrogen generation in fuel cell applications. *Control Engineering Practice*, 14(3):277–293, 2006.

[24] Colleen Spiegel. *PEM Fuel Cell Modeling and Simulation using MATLAB.* Academic Press, 2011.

[25] D Cheddie and N Munroe. Review and comparison of approaches to proton exchange membrane fuel cell modeling. *Journal of Power Sources*, 147(1):72–84, 2005.

[26] J Garnier, M C Pera, D Hissel, F Harel, D Candusso, N Glandu, J P Diard, A De Bernardinis, J M Kauffmann, and G Coquery. Dynamic PEM fuel cell modeling for automotive applications. In *Vehicular Technology Conference, 2003. VTC 2003-Fall. 2003 IEEE 58th.* vol. 5, pp. 3284–3288. IEEE, 2003.